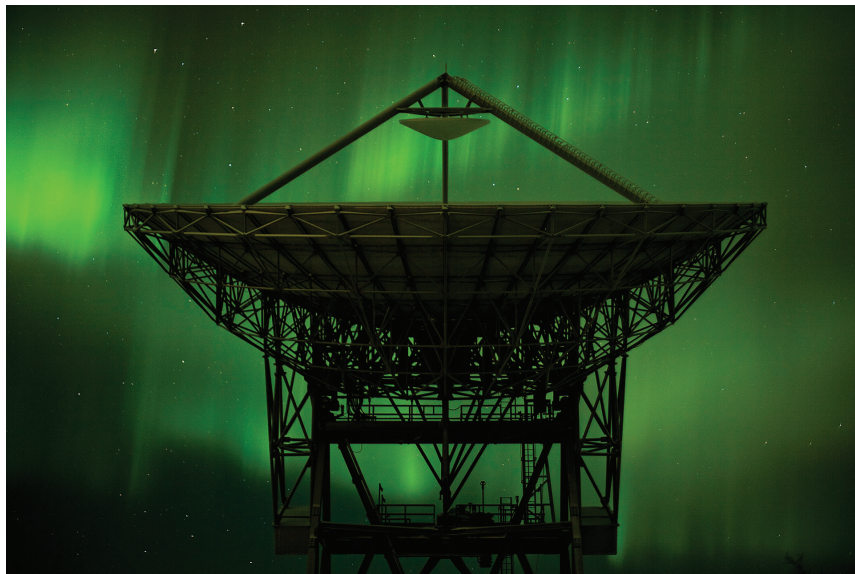


45th Annual European Meeting on Atmospheric Studies by Optical Methods



Lars-Göran Vanhainen

27-31 August 2018

**Swedish Institute
of Space Physics,
Kiruna, Sweden**



Peter Dalin

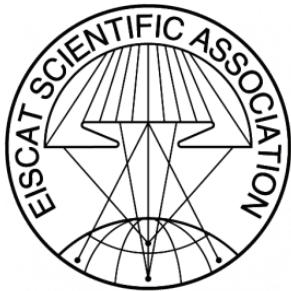
Uwe Raffalski



45AM is supported by:



Swedish Institute of Space Physics
Box 812
SE-981 28 Kiruna
Sweden
www.irf.se



EISCAT Scientific Association
Box 812
SE-981 28 Kiruna
Sweden
www.eiscat.se



SSC
Esrange Space Center
Box 802
SE-981 28 Kiruna
www.sscspace.com



Varsiti program (Variability of the Sun and
Its Terrestrial Impact) Scientific Committee
on Solar-Terrestrial Physics (SCOSTEP)
www.varsiti.org/

with support from the Swedish Research Council, VR

**45th Annual European Meeting
on Atmospheric Studies
by Optical Methods**

27-31 August 2018

**Swedish Institute of Space Physics,
Kiruna, Sweden**

Scientific Programme Committee

Tima Sergienko, Swedish Institute of Space Physics, Kiruna, Sweden (chair)
Urban Brändström, Swedish Institute of Space Physics, Kiruna, Sweden
Johan Kero, Swedish Institute of Space Physics, Kiruna, Sweden
Michael Gausa, ALOMAR Observatory, Andøya Space Center, Andenes, Norway
Björn Gustavsson, UIT, the Arctic University of Norway, Tromsø Norway
Fred Sigernes, UNIS, Longyearbyen; Birkeland Centre for Space Science (BCSS), University of Bergen; The Kjell Henriksen Observatory, Svalbard; and Centre for Autonomous Marine Operations and Systems, NTNU, Norway
Mike Taylor, Utah State University, USA
Oscar van der Velde, Polytechnic University of Catalonia, Terrassa, Spain
Daniel Whiter, University of Southampton, UK

Local Organising Committee (45AM LOC)

Tima Sergienko, Swedish Institute of Space Physics (IRF), chairman of the LOC
Urban Brändström, IRF
Carl-Fredrik Enell, EISCAT Scientific Association
Daria Mikhaylova, IRF
Rick McGregor, IRF
Annelie Klint Nilsson, IRF
Maria Wästle, IRF
Mats Luspa, IRF
Kent Andersson, SSC Esrange Space Center

45AM LOC address

Swedish Institute of Space Physics
Box 812
SE-981 28 Kiruna
Sweden
tel. +46-980-79000
fax +46-980-79050
e-mail: 45am@irf.se
internet: <https://45am.irf.se>

CONTENTS

Aurora and ionosphere-thermosphere interaction

<u>Bag, T.</u> , T. Sergienko and U. Brandstrom. N ₂ 1P Auroral Emission: Modeling and preliminary result. (Poster)	7
Belakhovsky, V.B., Y. Jin and W.J. Miloch. Influence of different ionospheric disturbances on the GPS scintillations at high latitudes.	8
Clausen, L.B.N., H. Nickisch and <u>A. Spicher</u> . Automatic classification of auroral images from the Oslo Auroral THEMIS (OATH) dataset using machine learning.	9
Chernous, S, <u>P. Budnikov</u> , I. Shagimuratov, V. Alpatov, M. Filatov, I. Efshov and N. Tepenitsina. Variations of GNSS signals in Euro-Arctic region during auroral activity.	10
<u>Dashkevich Zh.V.</u> and V.E. Ivanov. The evaluation of the NO density in the polar region using the ground-based photometer data. (Poster)	11
Gustavsson. B. Flickering Aurora: time-dependent electron transport modelling of electron precipitation at 5-12 Hz.	12
<u>Kozelov B.V.</u> , V.E. Ivanov and Z.V. Dashkevich. Triangulation of altitude profiles of auroral emission by MAIN system in Apatity.	13
<u>McKay, D.</u> , T. Paavilainen, B.Gustavsson, A. Kvammen and N. Partamies. Lumikot: fast auroral transients.	14
<u>Partamies, N.</u> , J. Weygand and L. Juusola. Auroral omega bands.	15
<u>Partamies, N.</u> , D. Whiter, K. Bolmgren, A. Kadokura and K. Kauristie. Pulsating aurora — why should we care?	16
<u>Price, D.</u> , D. Whiter and J. Chadney. A new technique for measuring heating of the lower thermosphere by auroral processes.	17
<u>Reidy, J. A.</u> , R. C. Fear, D. K. Whiter, B. S. Lanchester and A. J. Kavanagh. Multi-scale observation of polar cap aurora.	18
Sergienko, T. The fast variable aurora: Results of the Monte-Carlo simulation.	19
Sigernes, F. An update on the mobile app: The Aurora Forecast 3D.	20
<u>Vasilyev, R.</u> , M. Artamonov, A. Beletsky, M. Klimenko, A. Mikhalev, K. Ratovsky and G.Zherebtsov. Aurora, wind and temperature of mid-latitude upper atmosphere during geomagnetic perturbations.	21
<u>Whiter, D.</u> , H. Dahlgren, B. S. Lanchester, F. J. Mulligan, S. Rourke, J.Kealy, N.Ivchenko and J.M.Chadney, Optical emission produced by a combination of infra-sound and an auroral electric field?	22
<u>Yamauchi, M.</u> , U. Brändström, D. van Dijk, S. Kosé, M. Nishi, P. Wintoft and T. Sergienko. Automatic processing of combined ground-based measurements. (Poster)	23
Zhou, X. Dayside auroral dynamics under interplanetary shock conditions. (Invited)	24

Noctilucent clouds and mesospheric aeronomy

<u>Chadney, J.M.</u> , D.K. Whiter and B.S. Lanchester. Changes in hydroxyl temperatures during high-energy auroral precipitation. (Invited)	26
<u>Dalin, P.</u> , R. Latteck, I. Mann and I. Häggström. Common-volume observations of NLC and PMSE above Andoya. (Poster)	27
<u>Roldugin, V.C.</u> , S.M. Chernyakov, A.V. Roldugin and O.F. Ogloblina. Simultaneous observations of noctilucent clouds and polar mesospheric summer echoes at subauroral zone on 12 August 2016. (Poster presented by Kozelov)	28
<u>Stegman, J.</u> , J. Gumbel, L. Megner, O. M. Christensen, J. Hedin, M. Janghede, D. P. Murtagh, N. Ivchenko and the MATS Team. The MATS satellite - mission planning and optical calibration.	29
<u>Suzuki, H.</u> and Yamashita, R. Derivation of the horizontal wind field in the polar mesopause region by using successive images of noctilucent clouds from ground.	30
<u>Vasilyev, R.</u> , M. Artamonov, E. Devyatova, I. Medvedeva, E. Merzlyakov, A. Mikhalev, V. Mordvinov, A. Pogoreltsev and O. Zorkaltseva. Sudden stratospheric warming events 2017, 2018 and mesosphere over Eastern Siberia.	31

Atmospheric electricity (e.g. sprites, blue jets etc.)

<u>Garipov, G. K.</u> , M. I. Panasyuk, S. I. Svertilov, V. V. Bogomolov, V. O. Barinova and K. Yu. Saleev. Detection of Global Optical Phenomena of natural and man-made origin of Ultraviolet and Infrared glow of Earth atmosphere onboard the “Vernov” Satellite.	33
<u>Klimov, P.A.</u> , for the Lomonosov-UHECR/TLE Collaboration. The TUS detector on board the Lomonosov satellite: multi-functional geophysical UV observatory.	34
<u>Klimov, P.A.</u> , for the Lomonosov-UHECR/TLE Collaboration. UV transient emission of the atmosphere measured by the Lomonosov satellite with high temporal resolution.	35
<u>Klimov, P.A.</u> , M. A. Kaznacheeva, B. A. Khrenov, G. K. Garipov, V. V. Bogomolov, M.I. Panasyuk, S. I. Svertilov and R. Cremonini. UV transient atmospheric events observed far from thunderstorms by the Vernov satellite.	36
<u>van der Velde, O.</u> and J. Montanyà. Analysis of elves, Colombia gigantic jet campaigns, and the Atmosphere-Space Interactions Monitor.	37

Aerosol and clouds

<u>Groß, S.</u> , A. Ansmann, J. Gasteiger, V. Freudenthaler, M. Tesche, U. Wandinger and M. Wirth. Aerosol type classification and characterisation of microphysical parameters by lidar; challenges and technologies. (Invited)	39
---	----

<u>Tachikawa, M.</u> and Nakao, K. Optical trapping of ice crystals and its application in cloud physics	40
<u>Toledano, C.</u> , M. Gausa, C: Velasco, S. Blindheim, R. Román, I. Hanssen, D. Mateos, M. Herreras, R. González, A. Calle, V. E. Cachorro and A. M. de Frutos. Sun photometer and lidar collocated aerosol measurements at ALOMAR: a long-term comparison. (Invited)	41
<u>Voelger, P.</u> , and P. Dalin. Lidar observations at the Swedish Institute of Space Physics.	42
<u>Wolf, V.</u> , P. Voelger, T. Kuhn, M. Stanev and J. Gumbel. Synergies between balloon-borne in-situ particle imaging and ground-based lidar measurements of Arctic cirrus clouds.	43

Meteors

<u>Campbell-Brown, M.</u> , D. Subasinghe, D. Vida and T. Armitage. The Canadian Automated Meteor Observatory: high resolution studies of meteor ablation. (Invited)	45
<u>Kastinen, D.</u> , J. Kero, A. Pellinen-Wannberg, M. Holmström, J. Vaubailon and U. Brändström. A Monte-Carlo type simulation toolbox for small body dynamical astronomy. (Poster)	46
<u>Kero, J.</u> , D. Kastinen, G. Stober, C. Schult, P. Brown, Z. Krzeminski, R. Marshall, W. Cooke and I.Häggström. Simultaneous radar head echo and optical meteor observations.	47
<u>Ohsawa, R.</u> , S. Sako, F. Usui, Y. Sarugaku, M. Sato, Y. Fujiwara, T. Ootsubo, S. Abe, A. Hirota, K.Arimatsu, T. Kasuga, J. Watanabe and Tomo-e Gozen project. Members. Optical observations of faint meteors with a wide-field CMOS camera Tomo-e Gozen. (Invited)	48

Active experiments in the upper atmosphere

<u>Holmes, J.M.</u> , R. A. Dressler, T. R. Pedersen, R. G. Caton and D. Miller. A combined spectroscopic and plasma chemical kinetic analysis of ionospheric samarium releases. (Invited)	50
<u>Pedersen, T.</u> , J. Holmes and R. Caton. Spatial separation of optical spectral features in chemical release experiments. (Invited)	51

Ground-based, in-situ and space-based instruments, new facilities

<u>Alpatov, V.</u> , <u>P. Budnikov</u> and A. Vasiliev. Russian ionosphere monitoring system based on GNSS data. (Poster)	53
<u>Gulbrandsen, N.</u> , M. G. Johnsen, J. Matzka, U.-P. Hoppe, A. Serrano, P.D. Hillman and C.A.Denman. Laser investigation of the mesospheric magnetic field – The Mesospheric Sodium Layer as a Remotely, Optically Pumped Magnetometer. (Invited)	54

<u>Hanssen, I.</u> and M. Gausa. ALOMAR Tropospheric Lidar – Developments and ongoing projects. (Invited)	55
<u>Hirahara, M.</u> , Y. Saito, H. Kojima and M. Yamauchi. Japanese Space-Earth Coupling Exploration Mission by Multiple Polar-orbiting Compact Satellites and its Collaborations in Instrumentations and Ground-based Observations.	56
<u>Kealy, J.</u> and F. Mulligan. Detection of infrasound in the Earth’s upper atmosphere by observing nightglow emissions.	57
<u>Kieu, N.</u> , M. Passas, J. Sánchez and F. J. Gordillo-Vázquez. A quantitative analysis of high-speed time-resolved spectroscopy of sparks recorded by GALIUS. (Poster)	58
<u>Passas, M.</u> , N. Kieu, J. Sánchez, F. J. Gordillo-Vázquez, O. Van der Velde and J. Montanyá. GRASSP and GALIUS: two slit spectrographs designed to remotely characterize transient atmospheric plasmas. (Invited)	59
<u>Saito, Y.</u> , Y. Ogawa, H. Kojima, and SS-520-3 Sounding Rocket Experiment Team, SS-520-3 Sounding Rocket Experiment Targeting the Ion Outflow over the Cusp Region. (Invited)	60
<u>Sakanoi, T.</u> , <u>M. Hirahara</u> , M. Yamauchi, K. Asamura, Y. Saito, Shin-ichiro Oyama, H. Kojima, N. Kitamura, Yuichi Tsuda, A. Matsuoka, Y. Miyoshi, K. Hosokawa, N. Yagi and M. Fuiizawa. FACTORS: A future satellite mission for understanding the coupling and transportation processes in the upper atmosphere. (Poster)	61
<u>Sigernes, F.</u> , M. Syrjäsuo, R. Storvold, J. Fortuna, M. E. Grøtte, J. Veisdal, E. Honoré-Livermore and T. A. Johansen. The DIY hyperspectral imager experiment.	62
<u>Spicher, A.</u> , J. I. Moen, H. Hoang, K. Røed, E. Trondsen, L. B. N. Clausen and W. J. Miloch. The Investigation of Cusp irregularities 5 sounding rocket: multipoint measurement of turbulence. (Invited)	63
<u>Vasilyev, R.</u> , A. Beletsky, A. Bogomolov, M. Kaznacheeva, P. Klimov, E. Komarova, A. Mikhalev, R. Rakhmatulin, S. Podlesny and I. Tkachev. Coordinated satellite and ground-based observations of fast atmospheric processes.	64
<u>Zhou, X.</u> and S. B. Rafol. Development of a near-infrared balloon-borne camera for dayside and sunlit auroral observations.	65

EISCAT-3D and optical instruments

<u>Brändström, U.</u> , the ALIS_4D team, the KAGO team and the EWOC team. ALIS_4D, a Swedish complementary instrument for EISCAT_3D, status of Kiruna Atmospheric and Geophysical Observatory and the European Working group on optical calibration.	67
<u>Enell, C.-F.</u> , H. Hellgren, C. J. Heinselman, A. Westman and J. Markkanen. EISCAT 3D: overview of the system and its experiment modes.	68
Heinselman, C. EISCAT_3D Capabilities and Status. (Invited)	69
<u>Oyama, S.</u> , M. G. Conde, A. Aikio, E. Turunen, K. Kauristie, H. Vanhamäki, I. Virtanen, U. Brändström, T. Ulich, L. Cai, A. Workayehu, K. Shiokawa, M. Ishii, M. Hirahara, T. Sakanoi, Y. Tanaka, C. Fallen, B. J. Watkins, M. Orispää and Y. Ogawa. New insights found from coalescence of the ionospheric and thermospheric measurements at auroral latitudes.	70

Ulich, T., S. Oyama, U. Brändström, K. Kauristie, B. Gustavsson and C. Hall. Optical and other ground-based instrumentation: readiness for EISCAT_3D.

71

Aurora and ionosphere-thermosphere interaction

Poster

N₂ 1P auroral emission: modeling and preliminary result

Tikemani Bag¹, T. Sergienko¹ and U. Brändström¹

(1) Swedish Institute of Space Physics, Kiruna, Sweden

The vibrational distribution of N₂ triplet systems in aurora is of considerable interest because the band emissions resulting from these states carry information about the atmospheric composition, structure, dynamics and electron flux. Earlier steady state model for N₂⁺ 1N emission has been successfully applied to (1) evaluate electron excitation cross sections for N₂ ions from simultaneous measurements of blue line emission and precipitating electron flux and (2) analyse the Reimei particle and optical data. Beholding the successful implementation of earlier model, we have developed a time dependent model that can have a versatile applicability. The significance of the present time dependent model is that it calculates the population of different vibrational states of N₂ triplet manifold by solving their continuity equations. It incorporates all the known reaction mechanisms including electronic impact excitation, radiative and intra-system cascade, electronic quenching and inter-system collisional transfer (ICT). The reaction rate coefficients, cross-sections and electron flux are obtained from latest theoretical studies and experimental observations. The model is validated using data from ground based and space borne observations such as Auroral Large Imaging System (ALIS) and Reimei satellite. The approach here is to select appropriate observations from the data available, from which emission rates and population of different vibrational levels will be determined. Initially the present model would be applied to study N₂ first positive emission in a similar way to earlier steady state mode for blue line emission. Then the population of N₂(A) state would be used to investigate the green line auroral emission. It is because the energy transfer from N₂(A) state to atomic oxygen is one of the important excitation mechanisms for the production of auroral green line emission.

Regular

Influence of different ionospheric disturbances on the GPS scintillations at high latitudes

V.B. Belakhovsky¹, Y. Jin² and W.J. Miloch²

(1) Polar Geophysical Institute, Apatity, Russia

(2) Department of Physics, University of Oslo, Oslo, Norway

In this work we compare the influence of auroral particle precipitation and polar cap patches (PCP) on scintillations of the GPS signals in the polar ionosphere. We use the GPS scintillation receivers at Ny-Ålesund, operated by the University of Oslo. The presence of the auroral particle precipitation and polar cap patches was determined by using data from the EISCAT 42m radar and optical aurora observations on Svalbard. We analyzed about 100 events for years 2010-2017, when simultaneous EISCAT 42m and GPS data were available. We consider the following types of the auroral precipitation: i) the dayside and morning precipitation, ii) precipitation on the nightside during substorms, iii) precipitation associated with the arrival of the interplanetary shock wave. All considered types of ionospheric disturbances lead to enhanced GPS phase scintillations. For the polar cap patches, the morning and daytime precipitation (i), and precipitation related to the shock wave (iii), the phase scintillations index reaches values less than 1 radian. We observe that auroral precipitation during substorms leads to the greatest enhancement of the phase scintillation index (up to 3 radians). Thus, the substorm precipitation has the strongest impact on the scintillation of GPS radio signals in the polar ionosphere.

Regular

Automatic classification of auroral images from the Oslo Auroral THEMIS (OATH) dataset using machine learning

Lasse B. N. Clausen¹, Hannes Nickisch² and Andres Spicher³

(1) Department of Physics, University of Oslo, Oslo, Norway

(2) Philips Research, Hamburg, Germany

Based on their salient features we manually label 5824 images from various THEMIS all-sky imagers; the labels we use are "clear/noaurora", "cloudy", "moon", "arc", "diffuse", and "discrete". We then use a pre-trained deep neural network to automatically extract a 1001-dimensional feature vector from these images. Together, the labels and feature vectors are used to train a ridge classifier that is then able to correctly predict the category of unseen auroral images based on extracted features with 82% accuracy. If we only distinguish between a binary classification "aurora" and "no aurora", the true positive rate increases to 96%. While this study paves the way for easy automatic classification of all auroral images from the THEMIS all-sky imager chain, we believe that the methodology shown here is readily applied to all images from any other auroral imager as long as the data is available in digital form. Both the neural network and the ridge classifier are free, off-the-shelf computer codes; the simplicity of our approach is demonstrated by the fact that our entire analysis comprises about 50 lines of Python code. Automatically attaching labels to all available all-sky imager data would enable statistical studies of unprecedented scope.

Regular

Variations of GNSS signals in Euro-Arctic region during auroral activity

S. Chernous¹, P. Budnikov², I. Shagimuratov³, V. Alpatov³, M. Filatov¹, I. Efishov² and N. Tepenitsina²

(1) Polar Geophysical Institute, Murmansk, Russia

(2) Kaliningrad department of IZMIRAN, Kaliningrad, Russia

(3) Fedorov Institute of Applied Geophysics Roscomhydromet, Russia

Space weather affects the transionosphere GNSS signals propagation. The ionosphere disturbances and scintillations in the auroral activity regions have great influence to the GNSS operability. To investigate the effect of the auroral activity on the GNSS, the data of the auroral activity and GNSS data were analyzed. Particularly, the data during a huge magnetic storm on March 17-18, 2015 when auroras were observed from the polar regions up to 55-60th parallel, were studied. The next data sets were processed: RoTI, S4, H-component magnetic field disturbance, optical measurements of aurora, GNSS accuracy and errors numbers. Ionosphere scintillation indexes RoTI and S4 were obtained from GNSS signal measurements for each satellite. This data were collected from GNSS receivers, optical aurora detectors and magnetometers located along the meridian from St. Petersburg to Tromso. There were found, that the intensity of both RoTI and magnetic disturbances during magnetic storm were changed at the same time at mid-latitudes and at northern stations. The RoTI level corresponds to the amplitude of the H-component of the geomagnetic field variations and the position of the auroral oval. Dependence between GNSS accuracy and ionosphere activity also was observed. The results show that disruptions in GNSS operation and large positioning errors can take place even in the middle latitudes during huge magnetic storms when the auroral oval moves toward the equator. In such cases the level of auroral activity can be used to estimate the GNSS operability and accuracy. Authors thanks to the RFBR grant 17-45-510341 for partial support of this work.

Poster

The evaluation of the NO density in the polar region using the ground-based photometer data.

Dashkevich Zh.V. and Ivanov V.E.

Polar Geophysical Institute, Apapity, Russia.

The effect of the nitric oxide NO on the 5577A emission intensity during electron polar aurora is studied. It is shown that the reaction region.

We show evidence of auroral omega bands being related to fast Earthward flows in the magnetotail and discuss a possible scenario of omega formation based on the results of this study.

Regular

Flickering Aurora: time-dependent electron transport modelling of electron precipitation at 5-12 Hz

B. Gustavsson¹

(1) UIT, the Arctic University of Norway, Tromsø Norway, bjorn.gustavsson@uit.no

Flickering aurora, where the intensity varies in complex spatio-temporal patterns at 5 – 15 Hz (typically), is one of several auroral phenomena where the dominant dynamics occur at time-scales shorter than the travel-time for energetic electrons from the source altitude to the ionospheric E-region. To properly model the interaction between the precipitation and the thermosphere/ionosphere it is necessary to take the time-variations into account for the electron transport. In this presentation we will show results from the first time-dependent multi-stream electron transport calculations. We compare the time and altitude variations of modeled volume-emission-rates from molecular nitrogen, molecular nitrogen ions and atomic oxygen excited by field-aligned bursts of electrons and fluxes of accelerated electrons with modulated flux, modulated acceleration-potential and pitch-angle distribution. The results are compared with multi-monochromatic observations of flickering aurora and test-implications and observational challenges are presented.

Regular

Triangulation of altitude profiles of auroral emission by MAIN system in Apatity

B.V. Kozelov, V.E. Ivanov and Z.V. Dashkevich

Polar Geophysical Institute, Khalturin str., 15, Murmansk, 183010 Russia,
boris.kozelov@gmail.com

The Multiscale Aurora Imaging Network (MAIN) system of auroral cameras has two identical synchronized digital cameras with diagonal field of view of 18 degrees [1]. The cameras are equipped with glass filters that separate the blue-green part of the visible spectrum [2]. The observation points are separated by 4 km in longitude, so it is possible to triangulate small-scale auroral forms. Here we analysed observations of auroral rays near local magnetic zenith. Identification of solitary rays in images from both cameras allows us to deduce the altitude profile of auroral emission [3]. The spectra of precipitating electron fluxes were estimated from these altitude profiles using a numerical model of electron degradation in the atmosphere [4-6]. It is concluded that the brightening in rayed forms is usually accompanied by a hardening of the spectra of precipitating electrons.

References

- [1] Kozelov B.V., Pilgaev S.V., Borovkov L.P., Yurov V.E., Multi-scale auroral observations in Apatity: winter 2010-2011 // Geosci. Instrum. Method. Data Syst., 1, 1-6, 2012, www.geosci-instrument-method-data-syst.net/1/1/2012/doi:10.5194/gi-1-1-2012.
- [2] Kozelov B.V., Brandstrom B.U.E., Sigernes F., Roldugin A.V., Chernouss S.A., Practice of CCD cameras' calibration by LED low-light source. // "Physics of Auroral Phenomena" – Apatity, 2013. - P. 151-154.
- [3] Dobrolenskiy Y. S., Kozelov B. V., Kuzmin A. K., Lyahov A. N., Maslov I. A., Merzlyi A.M., Pulinets S. A., Chernous S. A. Researches of Auroral Characteristics and Altitude-Latitude Emission Structures of the Earth's Upper Atmosphere and Ionosphere by Means of Space Reconstruction of Auroral Images Detected from the Orbit Perspective Microsatellite // In book: MECHANICS, MANAGEMENT AND INFORMATICS. – Moscow: IKI RAS, 2015. - ISSN: 2075-6836. - T.7. №4 (57). - P.77-90 (in Russian).
- [4] Sergienko T.I., Ivanov V.E. A new approach to calculate the excitation of atmospheric gases by auroral electron impact // Ann. Geophys. - 1993. - V.11. - P.717.
- [5] Ivanov V.E., Kozelov B.V. Transport of electron and proton-hydrogen fluxes in the Earth's atmosphere // Apatity: KSC RAS, 2001.- P.260 (in Russian).
- [6] Dashkevich Z.V., Kozelov B.V. Synthetic radiation spectra of some systems of blue-green spectral bands // "Physics of Auroral Phenomena" - Apatity, 2015. - P.123-126.

Regular

Lumikot: fast auroral transients

D. McKay¹, T. Paavilainen², B.Gustavsson¹, A. Kvammen¹ and N. Partamies^{3,4}

(1) UiT -- The Arctic University of Norway, Tromsø, Norway

(2) University of Helsinki, Helsinki, Finland

(3) UNIS University Centre in Svalbard, Svalbard, Norway

(4) Birkeland Centre for Space Science, Bergen, Norway

The growth phase of magnetospheric substorms is interesting as the dynamics are simpler than other phases. Thus, it is easier to separate and understand the physical processes before the complex interactions occur in the expansion and recovery phases. As a result of growth-phase studies, a type of fast discreet auroral transient phenomenon has been observed during substorm events. These are significant phenomenon in the growth-phase, and are indicative of complex conditions on the boundary between the outer radiation belt and the plasma-sheet. We report on the findings and present several example cases, explaining also the difficulties of the observations and the opportunities for future work.

Regular

Auroral omega bands

N. Partamies¹, J. Weygand² and L. Juusola³

(1) UNIS / Birkeland Centre for Space Science, Norway, noora.partamies@unis.no

(2) University of California, Los Angeles, USA

(3) Finnish Meteorological Institute, Helsinki, Finland

Omega band aurora has been described as a wave form of the boundary of diffuse aurora which resembles a Greek omega letter. These forms are related to auroral activity in the morning sector and to the substorm recovery phases. A number of detailed multi-instrument case studies have been reported on omega bands but very few statistical investigations have been performed, suggesting that omega forms are not very common in auroral displays.

MIRACLE all-sky camera data from five Lapland stations over 1996–2007 have been searched for omega structures. The diffuse aurora boundary undulations can be identified in the ASC keograms but only a fraction of them qualifies as omegas. We required a clear structure which was traceable for longer than a minute. We also required a structure being taller than wider and we required an eastward propagation for it. We found 458 omega-like structures in total, most of them at the southern part of the auroral oval, in the field-of-view of Sodankylä camera. All omega bands occurred after a substorm onset and most of them during a recovery phase. The substorms with omega bands were found to be more intense than average substorms within the Lapland region. Wave-like undulation was observed not only in the optical emission but also in the equivalent current distribution. Omega forms occurred within a westward electrojet current which appeared stronger than that of average substorms in the same region.

We show evidence of auroral omega bands being related to fast Earthward flows in the magnetotail and discuss a possible scenario of omega formation based on the results of this study.

Regular

Pulsating aurora — why should we care?

N. Partamies¹, D. Whiter², K. Bolmgren³, A. Kadokura⁴ and K. Kauristie⁵

(1) The University Centre in Svalbard / Birkeland Centre for Space Science, Norway,
noora.partamies@unis.no

(2) University of Southampton, UK

(3) University of Bath, UK

(4) National Institute of Polar Research, Tokyo, Japan

(5) Finnish Meteorological Institute, Finland

Pulsating aurora consists of irregular auroral shapes fluctuating between states of dim and bright luminosity with periods of seconds to tens of seconds. A variety of pulsation frequencies can be observed simultaneously and visual auroral intensities are generally weak. This type of auroral activity is typically observed during and beyond substorm recovery phases and within the morning sector aurora. Earlier studies show that the electron precipitation energy can reach relativistic level and the precipitation may thus affect the mesospheric chemistry. Pulsation within an auroral all-sky camera (ASC) field of view leaves a distinct trace in the quick look data (keograms available at <http://www.space.fmi.fi/MIRACLE/ASC/>) making the events relatively easy to identify.

In this study, MIRACLE ASC data from five Lapland stations in 1997–2007 have been used to analyse typical properties of auroral pulsations. Based on about 400 pulsating auroral events over the Fennoscandian Lapland we outline the typical duration, geomagnetic conditions and change in the peak emission height for the events. We show that the auroral peak emission height decreases by about 8 km on average at the start of the pulsation. For about 10% of the events this brings the auroral precipitation down to about 90 km suggesting electron precipitation energies of 10 keV and above. A conservative estimate of the median duration of auroral pulsations observed over Lapland is about 1.4 hours. A large portion of the pulsating aurora occurs on both hemispheres at the same time, which increases the atmospheric impact. A more detailed investigation of the patch size evolution within the pulsating aurora reveals a large variation in the patch size evolution but also a distinct behaviour of the extremes, i.e. monotonically increasing and decreasing patch sizes. Only the events with decreasing patch sizes associate with strong energisation of the electron precipitation. They largely occur after the recovery of the magnetic disturbances, which makes them invisible for the magnetic index based proxies of energetic precipitation. Further work is needed to observationally characterise the typical precipitation energies and the atmospheric effects related to pulsating aurora.

Regular

A new technique for measuring heating of the lower thermosphere by auroral processes.

D. Price¹, D. Whiter¹ and J. Chadney¹

(1) University of Southampton, University Road, Southampton, SO17 1BJ.

We present a new analysis method, combining a range of optical observations and techniques, to measure the extent at which auroral processes affect the neutral temperature in the lower thermosphere. The University of Southampton's Auroral Structure and Kinetics (ASK) instrument and the ESR (EISCAT Svalbard Radar) are used to measure the precipitating particle energies for a chosen auroral event at a high temporal resolution. These energies are then used as an input for the Southampton ionospheric model to retrieve N₂ volume emission rate profiles over the course of the event. The modelled N₂ volume emission rate profile is combined with a range of trial neutral temperature profiles to generate a large library of synthetic N₂ 1PG spectra. These spectra are then compared to the spectrum recorded by the University of Southampton's HiTIES (High Throughput Imaging Echelle Spectrograph) instrument to determine the most realistic temperature profile. The result is a time series of best fit temperature profiles at high cadence for the duration of the auroral event, allowing us to distinguish between the temperature changes due to variations in emission altitude and those due to localized heating.

Regular

Multi-scale observation of polar cap aurora

J. A. Reidy^{1,2}, R. C. Fear¹, D. K. Whiter¹, B. S. Lanchester¹ and A. J. Kavanagh²

(1) Department of Physics and Astronomy, University of Southampton, SO17 1BJ, UK

(2) British Antarctic Survey, Cambridge, CB3 0ET, UK

We present preliminary observations of a multi-scale polar cap arc event which occurred on 4th February 2016. Polar cap arcs are high latitude aurora occurring within the typically 'open' polar cap. This event was first identified using global scale images from the SSUSI (Special Sensor Ultraviolet Spectral Imager) instruments on board the DMSP (Defence Meteorological Satellite Program) spacecraft. This event consisted of multiple polar cap arcs seen over the Svalbard Archipelago where the University of Southampton has the Auroral Structure and Kinetics (ASK) instrument. ASK is world leading in the study of small scale aurora and consists of three high resolution multi-spectral cameras with a 6° field of view. We present global scale auroral observations from the DMSP SSUSI instrument, coupled with all-sky camera data and ASK observations of the fine-scale structure of the polar cap aurora to probe the multi-scale nature of this fascinating phenomenon.

Regular

The fast variable aurora: Results of the Monte-Carlo simulation

Sergienko, T.

(1) Swedish Institute of Space Physics, Kiruna, Sweden, tima@irf.se

Several types of the aurora such as pulsating, flickering, flaming auroras are characterized by very fast variations of the emission intensity. The time scale of these phenomena is frequently shorter than the characteristic time for which the electron transport process can be considered as stationary. Therefore, existing steady state models of the auroral electron transport can not be applied to study these phenomena. This report presents a first comprehensive time-dependent model for electron transport into Earth's thermosphere. The model is developed on the basis of a Monte Carlo simulation that allows to reproduce most adequately the stochastic nature of the electron interaction with atmospheric molecules and atoms.

Dependencies of the time-dependent characteristics of the electron transport on the characteristic energy, spectrum, pitch-angle distribution of the precipitating auroral electrons are presented.

Regular

An update on the mobile app: The Aurora Forecast 3D

F. Sigernes ^{1, 2, 3, 4}

- (1) University Centre in Svalbard (UNIS), N-9171 Longyearbyen, Norway
- (2) Birkeland Centre for Space Science (BCSS), University of Bergen, Norway
- (3) The Kjell Henriksen Observatory (KHO), Svalbard, Norway
- (4) Centre for Autonomous Marine Operations and Systems (AMOS), NTNU, Norway

The Aurora Forecast 3D is a cross platform tool to track down where the aurora is located in the sky from any location on planet. It renders Earth, planets and stars in 3 Dimensions (3D) with rotation and scaling in real time. The auroral forecasts are +0, +1 and +4 hours ahead in time based on the predicted Kp index from the Space Weather Prediction Centre (SWPC) at the National Oceanic and Atmospheric Administration (NOAA). New features are geomagnetic alert messages, 3-day space weather condition forecasts as news ticker and Two-Line Element (TLE) orbit calculations to visualize satellites in the 3D display.

Regular

Aurora, wind and temperature of mid-latitude upper atmosphere during geomagnetic perturbations.

R. Vasilyev¹, M. Artamonov¹, A. Beletsky¹, M. Klimenko,¹ A. Mikhalev¹, K. Ratovsky,¹
G. Zherebtsov¹

(1) Institute of Solar-Terrestrial Physics SB RAS, Russia, 664033, Irkutsk p/o box 291; Lermontov st., 126a, roman_vasilyev@iszf.irk.ru

Measurements of intensities and spectral features of atmospheric optical radiation during geomagnetic storms allow evaluate the significance of the events for atmosphere circulation and thermodynamic. Spectral analysis in couple with the all sky cameras allows watching both vertical and horizontal dynamic of the event. Finally usage of Doppler shifting analysis of the spectral lines get us the wind and temperature as important physical properties for building whole physical picture of the event. We present some selected results of upper atmosphere observations by complex of optical instruments (spectrographs, all-sky cameras, Fabry-Perot interferometers) placed at ISTP geophysical observatories. The work performed under financial support of RFBR grant 18-05-00594 A.

Regular

Optical emission produced by a combination of infra-sound and an auroral electric field?

D. K. Whiter¹, H. Dahlgren², B. S. Lanchester¹, F. J. Mulligan³, S. Rourke³, J. Kealy³, N.Ivchenko², J. M. Chadney¹

(1) University of Southampton, UK

(2) Royal Institute of Technology (KTH), Stockholm, Sweden

(3) Maynooth University, Ireland

We present observations of optical emission apparently associated with, but not part of, an auroral arc, recorded by the Auroral Structure and Kinetics (ASK) instrument close to Longyearbyen, Svalbard. The unusual emission forms several small (~3 km long) elongated structures aligned approximately perpendicular to the auroral arc, with approximately constant spacing between each of the structures giving the appearance of successive wave fronts. Each structure contains dynamic, smaller scale structure within, and moves in a direction approximately parallel to the auroral arc. Neither the main structures nor the sub-structure are aligned with the magnetic field. The ASK instrument consists of 3 co-aligned high-resolution EMCCD cameras each equipped with a different narrow passband interference filter to select emissions from N₂ 1PG (673.0nm), O (777.4nm) and O⁺ (732.0nm). The structures are predominantly seen in the N₂ 1PG emission, which has a lower activation energy than the O emission. The O⁺ emission is quenched at low altitude. Short periods of sporadic-E and intense electron heating were seen by the EISCAT Svalbard Radar coincidentally with the optical emission. We propose that the unusual optical features were caused by intense electric fields accelerating electrons horizontally across the magnetic field. We suggest that these intense electric fields were caused by a combination of the auroral arc and an infra-sound wave propagating parallel to the auroral arc. In this model the optical structures highlight regions where the electric fields from the arc and the infra-sound wave were parallel, while the gaps between the structures are regions where the electric fields from the two sources were anti-parallel. The motion of the structures correspond to the phase velocity of the infra-sound wave.

Poster

Automatic processing of combined ground-based measurements

M. Yamauchi¹, U. Brändström¹, D. van Dijk², S. Kosé³, M. Nishi⁴, P. Wintoft¹, T. Sergienko¹

(1) Swedish Institute of Space Physics, Sweden,

(2) The Hague University of applied science, The Netherlands (bachelor thesis work)

(3) Kyoto University, Japan (master student)

(4) Hiroshima City University, Japan

For both statistical studies and short-term forecast of auroral substorm/large ground induced current (GIC), automated identification of events of interest has long been performed by many methods. For short-term forecast, different types of data has been used for many years by experienced auroral scientists. However, automatic forecast using a combined data is not yet established.

To combine auroral image and magnetometer data, we propose to make "all-sky index" that characterizes different aurorae and their strengths as a simple index (a number or a set of numbers). The all-sky index must be very local depending on the camera city light, and latitude of the location. Here we show our attempt using Kiruna and Abisko all-sky cameras. For the magnetometer data, we try two different methods to estimate local GIC: one is gradient of peak-to-peak variation within a fixed window (dB/dt method), and the other is standard deviation (sd(B) method). Then we compared these methods to the substorm breakup or surge.

When we surveyed the strongest auroras during 2017, the peak of sd(B) is few minutes before the peak of dB/dt, which matches with the peak of all-sky index. This is not surprising because fluctuations often arrives before the large change in the magnetic field. If this is true, it opens up a possibility of few-minutes forecast. We present our algorithm and some examples.

Invited

Dayside auroral dynamics under interplanetary shock conditions

Xiaoyan Zhou^{1,2}

(1) Department of Earth, Planetary, and Space Sciences, University of California, Los Angeles, California, USA, xyzhou@igpp.ucla.edu

(2) XYZ Space Physics, Inc., Pasadena, California, USA

Interplanetary shocks are one of the most popular and well-studied heliospheric phenomena, at which the abrupt enhancement of the solar wind dynamic pressure can cause significant and global geo-effects. Different from solar wind pressure pulses and other solar wind transients, interplanetary shocks are well defined and described by theories and observations, such as the shock normal, shock angle, shock speed, shock Mach number, etc. Those characteristics predict the geo-effects in many ways, including the shock impact location on the magnetopause, the impact strength, and how fast the impact propagates along the magnetopause, even whether auroras will be generated or not. Therefore, there is less ambiguity when tracing an ionospheric disturbance back to the cause and driver in the magnetosphere, which can be tens of Earth radii away. The shock-generated aurora has transient, global, and dynamic significances. From space, auroral remote sensing in ultraviolet wavelengths revealed that the shock aurora first occurs around local noon, then propagates antisunward along the oval at a speed of ~6–11 km/s in the ionosphere. The propagation is also seen clearly in the enhancement of the ionospheric total electron content (TEC). In-situ observations from FAST and DMSP showed that precipitated low-energy electrons (in a few hundred eV) are along highly structured field-aligned currents at the poleward boundary of the oval, while the precipitated high-energy electrons (~> 1 keV) are highly isotropic filling the loss cone along the closed field lines. These observations predict that red auroral arcs are along the poleward boundary and the green diffuse aurora is along the main oval. The ground-based observations from ASI and MSP allowed further insight into the shock-aurora forms and unveiled the difference of the auroral dynamics between local noon and dawnside auroras. In the local noon sector (~09-15 MLT), auroral emissions in different colors occur at the same time, but in different forms at different locations, i.e., the discrete arcs are in red at high latitudes, and the diffuse aurora is in green at low latitudes, but they are illuminated at the same time. Around 6 MLT, auroral emissions in different colors occur at the same time, in the same forms, along the same magnetic fluxes, i.e., discrete auroras appear to be auroral streaks along the same flux illuminated with red at high altitudes with green and purple at low altitudes along the poleward boundary of the oval, diffuse auroras are seen in both red and green at the same low latitudes, and all forms are moving antisunward. Such auroral activity and dynamics strongly suggest that the precipitation mechanisms are - the adiabatic compression plus the magnetic reconnection near local noon, and the adiabatic compression plus velocity and magnetic shears as well as the Kelvin-Helmholtz instability at the dawnside magnetopause flank.

Noctilucent clouds and mesospheric aeronomy

Invited

Changes in hydroxyl temperatures during high-energy auroral precipitation

J.M. Chadney¹, D.K. Whiter¹, B.S. Lanchester¹

(1) Space Environment Physics Group, University of Southampton, UK, j.m.chadney@soton.ac.uk

Hydroxyl rotational temperatures can be derived from spectral measurements of the layer of excited OH molecules located at about 87 km altitude. To determine OH temperatures during periods of aurora, we have developed a spectral fitting method to separate OH airglow emissions from auroral O⁺ and N₂ in observations between 725 – 740 nm using the High Throughput Imaging Echelle Spectrograph (HiTIES), located at the Kjell Henriksen Observatory on Svalbard. During periods of high-energy auroral precipitation, we observe changes in OH temperatures of around 10 K associated with a decrease in the intensity of OH emission. Events displaying either an increase or a decrease in temperature are seen. These temperature changes could be due to a change in the altitudinal distribution of OH molecules, caused by the destruction of the upper part of the part of the OH layer in presence of energetic auroral precipitation. We determine the altitudes affected by auroral precipitation by estimating the energy of the precipitating particles using the ASK (Auroral Structure and Kinetics) instrument, co-located with HiTIES. The mechanism for the partial destruction of the OH layer is tested using temperature profiles recorded by the SABER instrument onboard the TIMED spacecraft.

Poster

Common-volume observations of NLC and PMSE above Andoya

P. Dalin¹, R. Latteck², I. Mann³, I. Häggström⁴

(1) Swedish Institute of Space Physics, Kiruna, Sweden, (pdalin@irf.se)

(2) Leibniz-Institute of Atmospheric Physics, Kühlungsborn, Germany

(3) Department of Physics and Technology, UiT the Arctic University of Norway, Tromsø, Norway

(4) EISCAT Scientific Association, Kiruna, Sweden

Ice particles form during summer months at the mesopause region (80-90 km) at middle to high latitudes. The ice particles form in optically visible noctilucent clouds (NLC) and cause the formation of specific radar echoes called polar mesospheric summer echoes (PMSE). While NLC and PMSE are both linked to the presence of ice particles and observed at similar overlapping altitudes, they are also influenced by other parameters, e.g. neutral atmospheric dynamics, turbulence and dusty plasma effects, and their exact formation conditions are still subject to investigations. We here present a unique case of simultaneous observations of both phenomena.

The “Mesoclouds” campaign has been conducted every August since 2015, aiming to investigate PMSE and NLC activity in the common volume of the atmosphere above the Tromsø EISCAT station. We simultaneously run optical and radar measurements: the EISCAT VHF radars located at Tromsø (Norway), Kiruna (Sweden) and Sodankylä (Finland), two optical NLC cameras located at Kiruna and Nikkaluokta (Sweden) as well as the MAARSY and ESRAD VHF radars located at Andoya (Norway) and Esrange (Sweden), respectively. The NLC cameras are separated by 60 km allowing triangulation measurements of NLC and hence estimating their heights and dynamic in 3D space. The NLC cameras are about 200 km south of Tromsø, which permits making common-volume observations of NLC and PMSE inside the EISCAT and MAARSY radar beams.

We have observed a unique case of simultaneous NLC and PMSE occurrences above northern Scandinavia on the night of 13-14 August 2017. Very bright and extensive NLC and PMSE layers were located very close to each others in space. The NLC layer was due to the area with low temperature at the summer mesopause located right above northern Scandinavia as demonstrated by Aura satellite measurements. The horizontal transport of air masses from NE to SW was a reason of sudden appearance of very bright and extensive NLC in the field of view of the cameras and inside the MAARSY radar beam. A clear anticorrelation behavior between the NLC brightness and PMSE strength was observed. Features of this simultaneous NLC and PMSE dynamical behavior are discussed in the present paper.

Poster

Simultaneous observations of noctilucent clouds and polar mesospheric summer echoes at subauroral zone on 12 August 2016

V.C. Roldugin¹, S.M. Chernyakov¹, A.V. Roldugin¹, O.F. Ogloblina¹

(1) Polar Geophysical Institute, Apatity, Russia

On 12 August 2016 the intensive noctilucent clouds were registered by the all-sky camera in Lovozero at Kola peninsula. They extended over the entire celestial hemisphere observed by the all-sky camera; all of them moved in the southern direction, and the clouds had a tenuous structure and showed gravity waves with spatial periods of 15–100 km. During the presence of noctilucent clouds polar mesospheric summer echoes (PMSEs) were recorded at heights of 83–86 km by the partial reflection radar on the PGI observatory in Tumanny. It was found that the presence of only noctilucent clouds in diagram of the antenna pattern of the radar is not sufficient for the appearance of PMSEs; noctilucent clouds must also have irregularities of several kilometers. The PMSE heights decreased with a velocity of 0.5 and 1.3 m/s.

Regular

The MATS satellite – mission planning and optical calibration

J. Stegman¹, J. Gumbel¹, L. Megner¹, O. M. Christensen¹, J. Hedin¹, M. Janghede¹, D. P. Murtagh², N. Ivchenko³, and the MATS Team

(1) Department of Meteorology (MISU), Stockholm University, Sweden, e-mail: jacek@misu.su.se

(2) Department of Earth and Space Sciences, Chalmers University of Technology, Göteborg, Sweden

(3) School of Electrical Engineering, Royal Institute of Technology (KTH), Stockholm, Sweden

The new Swedish satellite MATS (Mesospheric Airglow/Aerosol Tomography and Spectroscopy) is being prepared for launch in late 2019. MATS science questions concern structures and wave activity in the mesosphere. Primary measurement targets are O₂ Atmospheric Band airglow in the near infrared, and sunlight scattered by noctilucent clouds in the ultraviolet. The main instrumentation consists of a limb imager with six spectral channels and a nadir imager with one spectral channel. While tomography will provide horizontally and vertically resolved data, spectroscopy will allow analysis in terms of mesospheric composition, temperature and cloud properties. This presentation provides an updated overview of the mission. A particular focus will be on the characterization and calibration of the instruments, both pre-flight and in orbit.

Regular

Derivation of the horizontal wind field in the polar mesopause region by using successive images of noctilucent clouds from ground

Hidehiko Suzuki and Ryoma Yamashita¹

(1) Dept of physics, Meiji University, Kawasaki, Kanagawa, Japan, suzuhide@meiji.ac.jp

It is important to quantify amplitude of turbulent motion to understand the energy and momentum budgets and distribution of minor constituents in the upper mesosphere. In particular, to know the eddy diffusion coefficient of minor constituents which are locally and impulsively produced by energetic particle precipitations in the polar mesopause is one of the most important subjects in the upper atmospheric science. One of the straight methods to know the amplitude of the eddy motion is to measure the wind field with both spatial and temporal domains. However, observation technique satisfying such requirements is limited in this altitude. In this study, derivation of the horizontal wind field in the polar mesopause region by tracking the motion of noctilucent clouds (NLCs) is examined. NLCs are the highest cloud in the Earth which appears in a mesopause region during summer season in both polar regions. Since the vertical extent of NLC is sufficiently thin (~within several hundred meters in typical), the apparent horizontal motion observed from ground can be regarded as the result of transportation by the horizontal winds at a single altitude. For northern hemisphere case, occurrence of NLC is high during a period between 10 days before and 50 days after a summer solstice (the NLC season). In addition, NLCs are only visible during astronomical and nautical twilight times (i.e solar elevation between -18 and -6 degrees) from ground in sub-polar area (latitudes between 50°N and 60°N). By considering these constrains, the best latitude which gives the longest duration for NLC observation can be determined by a simple geometric calculations. Duration of twilight period is longest (~6.5 hours) at latitude 50N in the beginning of the NLC season. However, the best latitude for an NLC observation shifts towards higher latitude (up to 60N) in the end of the NLC season. For example, duration of the twilight is 6 hours in 60N while it is reduced to 3.5 hours in 50N at the end of NLC season. Therefore, if several camera systems are installed to cover latitudes between 50N and 60N, it is possible to deduce horizontal wind field with 6 hours duration per a day in the polar mesopause region during all the NLC season (~ 2 months). This consideration suggests possibility of the NLC tracking method which can infer the wind field in both spatial and temporal domains to reveal dynamics of the turbulences in the polar mesopause region.

In this presentation, initial results of wind field derivation by tracking a motion of noctilucent clouds (NLC) observed by a ground-based colour digital camera in Iceland is reported. The procedure for wind field estimation is simple and consists with 3 steps; (1) projects raw images to a geographical map (2) enhances NLC structures by using FFT method (3) determines horizontal velocity vectors by applying template matching method to two sequential images. In this talk, a result of the wind derivation by using successive images of NLC with 3 minutes interval and ~1.5h duration observed on the night of Aug 1st, 2013, will be reported as a case study.

Regular

Sudden stratospheric warming events 2017, 2018 and mesosphere over Eastern Siberia.

R. Vasilyev¹, M. Artamonov¹, E. Devyatova¹, I. Medvedeva¹, E. Merzlyakov², A. Mikhalev¹, V. Mordvinov¹, A. Pogoreltsev³, O. Zorkaltseva¹

(1) Institute of Solar-Terrestrial Physics SB RAS, Russia, 664033, Irkutsk p/o box 291; Lermontov st., 126a, roman_vasilyev@iszf.irk.ru

(2) Institute of experimental meteorology, Roshydromet

(3) Russian State Hydrometeorological University

We present results of wind and temperature observations in the mesosphere and lower thermosphere region over Eastern Siberia using optical and radiophysical methods. We compare the empirical data with Middle/Upper Atmosphere Model (MUAM) in selected point and found the difference between them in terms of planetary tides. Two observed events differ by the position of main impact of sudden stratospheric warming events relatively to observational point so we have different pictures of the event. Nevertheless the results are in agreement with modern representations of the SSW events and they exhibit potential for further development of the model and method for data analysis.

Atmospheric electricity (e.g. sprites, blue jets etc.)

Regular

Detection of Global Optical Phenomena of natural and man-made origin of Ultraviolet and Infrared glow of Earth atmosphere onboard the “Vernov” Satellite

G. K. Garipov, M. I. Panasyuk, S. I. Svertilov, V. V. Bogomolov, V. O. Barinova,
K.Yu.Saleev

Skobeltsyn Institute of Nuclear Physics, Moscow State University, Moscow, 119234
Russia, ggkmsu@yandex.ru

The generation of transients in the Earth's upper atmosphere under the action of electron fluxes and high- and low-frequency electromagnetic waves has been studied onboard the small “Vernov” spacecraft (solar synchronous orbit, 98° inclination, height 640–830 km).

Main studies were carried out with ultraviolet (UV, 240–380 nm), red–infrared (IR, 610–800 nm), gamma-ray (0.01–3 MeV), and electron (0.2–15 MeV) detectors as well as with high-frequency (0.05–15 MHz) and low-frequency (0.1 Hz–40 kHz) radio receivers.

It is shown that on the night side in the middle latitudes man-made technogenic glow is observed along the selected meridians, whose distribution corresponds to the longitude of the most powerful low-frequency radio stations. The geographical distribution of this glow sharply changes at the border of the day and night side of the satellite's orbit, as a result of which on the day side such meridians are not allocated, and their geographical longitude distribution becomes uniform.

Light flashes caused by lightning discharges were also considered. It is shown that on the night side of the Earth the geographical distribution of flashes coincides with the global distribution of lightning. On the day side, light flashes are recorded much less frequently, and mainly in the polar regions of the Earth, the recording frequency of which does not depend of the local season of year.

Regular

The TUS detector on board the Lomonosov satellite: multifunctional geophysical UV observatory

P.A. Klimov¹, for the Lomonosov-UHECR/TLE Collaboration

(1) Skobeltsyn Institute of Nuclear Physics of Lomonosov Moscow State University, 1(2), Leninskie gory, GSP-1, Moscow 119991, Russian Federation, pavel.klimov@gmail.com

TUS (Tracking Ultraviolet Set-up) is an orbital imaging telescope of UV atmospheric radiation. It was launched into orbit on April 28, 2016, as a part of the scientific payload of the Lomonosov satellite to the solar-synchronous orbit 500 km of height. The field of view of the detector in the atmosphere is $80 \times 80 = 6400 \text{ km}^2$ with spatial resolution in the atmosphere of 5 km. Photo receiver of the detector is composed of 256 Hamamatsu PMTs sensitive in near UV wavelength band (240-400 nm). The TUS detector has several modes of operation with different temporal resolution (0.8 μs , 25.6 μs , 0.4 ms and 6.6 ms).

Having high sensitivity, spatial resolution and several modes of operation the TUS detector has been used as a unique UV geophysical observatory. A variety of different phenomena started to be studied by measuring ultraviolet signal from the atmosphere: extensive air showers from the ultrahigh energy cosmic rays, lightning discharges, transient atmospheric events, far-from-thunderstorm UV flashes, aurora ovals and meteors. Examples of measured events are presented and advantages of space-based observation are discussed.

Regular

UV transient emission of the atmosphere measured by the Lomonosov satellite with high temporal resolution

P.A. Klimov¹, for the Lomonosov-UHECR/TLE Collaboration

(1) Skobeltsyn Institute of Nuclear Physics of Lomonosov Moscow State University, 1(2), Leninskie gory, GSP-1, Moscow 119991, Russian Federation, pavel.klimov@gmail.com

The detector TUS (Tracking Ultraviolet Set-up) was launched into orbit on April 28, 2016, as a part of the scientific payload of the Moscow State University satellite Lomonosov. It is a UV sensitive telescope looking into the atmosphere from the altitude of ~500 km in nadir direction. This telescope has 5 km spatial resolution on the sea level and very high temporal resolution (up to 0.8 μ s). This allows one to study the atmospheric events which develop in the atmosphere at a speed of light. Among them are extensive air showers generated by the ultrahigh energy cosmic rays and arc-shaped fast developed discharges in the ionosphere: ELVES, related to the thunderstorm activity. The fine structure of various phenomena is measured. In particular, a complex time spatial structure of ELVES, consisting of several rings, has been observed and its relation to the compact intra cloud discharges was supposed.

The analyses of different events, their classification, comparison with the ground based observations (WWLLN and Vaisala GLD360 lightning location networks) and discussion of possible sources are presented. The work was done with partial financial support from the Russian Foundation for Basic Research grant 17-05-00492.

Regular

UV Transient Atmospheric Events Observed Far from Thunderstorms by the Vernov Satellite

P. A. Klimov¹, M. A. Kaznacheeva^{1,2}, B. A. Khrenov¹, G. K. Garipov¹, V. V. Bogomolov^{1,2}, M. I. Panasyuk^{1,2}, S. I. Svertilov^{1,2}, R. Cremonini³

(1) Skobeltsyn Institute of Nuclear Physics of Lomonosov Moscow State University, 1(2), Leninskie gory, GSP-1, Moscow 119991, Russian Federation, pavel.klimov@gmail.com

(2) Physical Department of Lomonosov Moscow State University, 1(2), Leninskie gory, GSP-1, Moscow 119991, Russian Federation

(3) Department of General Physics "A. Avogadro," University of Turin, 10125 Turin, Italy

Usually a thunderstorm region with lightning activity is necessary for the formation of known types of upper atmospheric transient luminous events (TLEs: sprites, elves, blue jets etc.) with well recognizable visible emissions. However, some "far-from-thunderstorm" transient events have been detected in some experiments. Measurements of transient atmospheric events were made on board the Vernov satellite by the sensitive UV and IR detector in 2014. These observations provided measurements all over the globe and allowed us to study events associated with thunderstorms (lightning, TLEs) and unusual UV flashes (UV transient atmospheric events, TAEs) far from thunderstorm regions. More than 8500 UV TAEs were measured by the Vernov satellite over the globe. Forty seven far-from-thunderstorm TAEs were selected having no lightning discharges during one hour in a radius of 1000 km around the location of the event according to the World Wide Lightning Location Network (WWLLN) and Vaisala Global Lightning Dataset (GLD360) data. Special attention was given to six events with complicated temporal structure and low luminosity in the IR channel. Their properties and atmospheric conditions were studied in details. The analysis of cloud cover in addition to the lightning location networks data demonstrated the low probability of any lightning in the region of measurements. These far-from-thunderstorm transient events are considered to be a new type of UV transient events in the atmosphere, without connection to the presence of thunderstorm activity in the region of observation. The mechanism of such transient emission is not clear yet. The work was done with partial financial support from the Russian Foundation for Basic Research grant 17-05-00492.

Regular

Analysis of elves, Colombia gigantic jet campaigns, and the Atmosphere-Space Interactions Monitor

O. van der Velde¹ and J. Montanyà¹

(1) Lightning Research Group, Electrical Engineering Department, Polytechnic University of Catalonia, Colon 1, Terrassa, Spain. oscar.van.der.velde@upc.edu

We summarize the imaging devices, campaigns and observations by the UPC Lightning Research Group in 2018. The main topics are elves, sprites and gigantic jets and simultaneous observations by the new Atmosphere-Space Interactions Monitor (ASIM) payload in orbit on the International Space Station, launched on April 2nd 2018.

Elves are very large circular optical emissions in the mesosphere, excited by the strongest of cloud-to-ground lightning strokes. Our statistics of elve altitudes presented at 43AM show them to occur at 87 km altitude with daily and hourly variations of a few kilometers. Images also show that atmospheric gravity waves can be observed as banding patterns in elves. Background images may reveal simultaneous banding in airglow. In early 2018, we continued to study this phenomenon by excluding most other airglow wavelengths than OH* which radiates across the near-infrared range. A 720 nm filter was mounted and images were taken at exposure times of 1 second by a sensitive camera. Backgrounds are assembled and subtracted from the image with elve, allowing comparison.

The second topic are the campaigns of 2017 and 2018 in Colombia to observe gigantic jets using intensified high-speed cameras. Two GJs were analyzed in detail from the 2017 campaign. In 2018, a new campaign is planned, for which we consider the Páramo de Santurban, near Bucaramanga, at 3300-3500 m above sea level. A simple camera will be installed soon to monitor night sky conditions during the wet season.

The third topic are the first ASIM results. It contains two instruments, the Modular Multispectral Imaging Array (MMIA) and Modular X-ray and Gamma-ray Sensor (MXGS) The MMIA contains filtered photometers and cameras for detection of transient luminous events. MXGS detects and quantifies terrestrial gamma-ray flashes and locates their producing lightning flashes by use of a coded mask. ASIM is complemented by the new ISS-LIS lightning imaging sensor. The first results are currently being obtained.

Aerosol and clouds

Invited

Aerosol type classification and characterisation of microphysical parameters by lidar; challenges and technologies

S. Groß¹, A. Ansmann², J. Gasteiger³, V. Freudenthaler⁴, M. Tesche⁵, U. Wandinger², M. Wirth¹

(1) German Aerospace Center (DLR), Institute of Atmospheric Physics, Münchener Str. 20, 82234 Wessling, Germany, silke.gross@dlr.de

(2) Leibniz Institute for Tropospheric Research (TROPOS), Permoser Str. 15, 04318 Leipzig, Germany

(3) University of Vienna, Aerosol Physics and Environmental Physics, Boltzmannngasse 5, 1090 Wien, Austria

(4) Ludwig-Maximilians-Universität, Meteorological Institute, Theresienstr. 37, 80333 München, Germany

(5) University of Herfordshire, Hatfield, United Kingdom

Light detection and ranging (lidar) has a long history in profiling the Earth's atmosphere. With its capability to identify and localize scattering layers with high spatial and temporal resolution it contributed significantly to our understanding of the Earth's atmosphere. Ceilometers, simple low power one wavelength systems, are frequently used in networks to monitor cloud base height as well as location and distribution of aerosol layers. Advanced lidar systems like high spectral resolution lidars (HSRL) or Raman lidars provide not only information about the location of the aerosol and cloud layers but direct measurements of the extinction coefficient profile of aerosol and ice cloud layers. If lidars have multi-wavelength and/or depolarisation sensitive capabilities they furthermore provide information that can be used to distinguish between different aerosol and cloud types, and to derive estimates of the microphysical properties of the aerosol, the contribution of different aerosol types to mixtures, and the estimation of aerosol mass concentration.

We will give an overview of the lidar principle and how it can be used for aerosol typing and to estimate microphysical aerosol properties.

Regular

Optical trapping of ice crystals and its application in cloud physics

Maki Tachikawa and Kotaro Nakao

Department of Physics, Meiji University, 1-1-1 Higashimita, Tama-ku, Kawasaki 214-8571, Japan
e-mail: tachikaw@meiji.ac.jp

Optical trapping, also known as optical tweezers, levitates a microparticle in air by use of radiation pressures from laser beams. We have developed an optical trap for micron-sized ice crystals to open a way to new experiments of cloud microphysics.

Our trap uses two counter-propagating Gaussian beams from a 532 nm Nd:YVO₄ laser [1]. It is installed in an open cold chamber which could be cooled from room temperature down to -50 °C. Figure 1 is a top view of the cold chamber showing an optically levitated single ice crystal. Morphology and size of the trapped particle are confirmed from scattering pattern of the trapping laser beams and microscope images; ice crystals are hexagonal plates with a diameter of a few tens microns.

This optical trap enables in situ observation of collision processes of ice crystals and supercooled water droplets, which are essential in cloud formation. A projectile particle is driven by the optical radiation pressure and directed towards a trapped particle. A high-speed microscope camera has recorded the moment of freezing of a supercooled water drop on contact with an ice crystal. Aggregations of colliding ice crystals and head-on collisions have also been observed.

We aim to clarify collision-induced electrification of ice crystals for a better understanding of the thundercloud electrification. Polarity of electrification can be determined by specifying the size and orientation of colliding crystals. So far, we observed several tens collision events, but no electrification occurred.

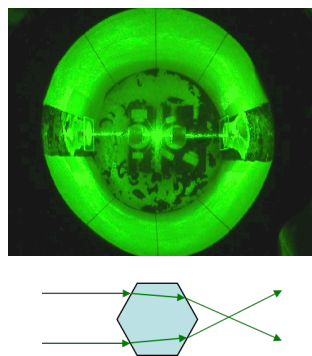


Fig. 1. Optically trapped ice crystal and deflected laser beams.

[1] K. Taji, M. Tachikawa, K. Nagashima, *Appl. Phys. Lett.* **88**, 141111 (2006).

Invited

Sun photometer and lidar collocated aerosol measurements at ALOMAR: a long-term comparison.

C. Toledano¹, M. Gausa², C. Velasco¹, S. Blindheim², R. Román¹, I. Hanssen², D. Mateos¹, M. Herreras¹, R. González¹, A. Calle¹, V. E. Cachorro¹, A. M. de Frutos¹,

(1) Group of Atmospheric Optics, University of Valladolid, Spain, toledano@goa.uva.es

(2) ALOMAR Observatory, Andøya Space Center, Andenes, Norway

Aerosols play a complex role in the atmospheric processes and their impact on radiation has the largest uncertainty in the changing radiative budget. Moreover, the aerosol characterization and typing is of great importance for satellite retrieval validation, especially at high latitudes where ground-based observations are scarce. In addition, modelling studies indicate that climate effects are enhanced at Arctic latitudes (Arctic amplification). In this context, the University of Valladolid and the Andøya Space Center carry out a long-term program for aerosol monitoring at ALOMAR Observatory (69N, 16E), located in Andøya island, Norway. Sun/Sky photometer measurements in the framework of AERONET have been used since 2002 to provide column aerosol optical depth and a set of optical and microphysical aerosol properties. Furthermore, collocated lidar observations for aerosol profiling in the troposphere have been carried out since 2006 in the framework of EARLINET. Both instruments were enhanced in the last years with major upgrades in the lidar system and the addition of direct Moon irradiance measurements in the photometer since 2015. The synergy between collocated lidar and Sun-Sky-Moon photometer observations allow a reliable columnar and vertically-resolved aerosol characterization, by means of inversion algorithms like GRASP, that perform joint inversion (lidar+photometer) for retrieval of advanced aerosol products. In addition to the long-term characterization, the analysis of particular events of long-range transported aerosol is also carried out.

Regular

Lidar observations at the Swedish Institute of Space Physics

P. Voelger¹, P.Dalin¹

(1) Swedish Institute of Space Physics (IRF), Box 812, 98128 Kiruna, Sweden, peter.voelger@irf.se

The lidar system at the Swedish Institute of Space Physics has been operated since several years now. Observation targets have been cirrus clouds in the troposphere and Polar Stratospheric clouds in the stratosphere. The presentation will show examples for both kind of measurements and interpret them.

Regular

Synergies between balloon-borne in-situ particle imaging and ground-based lidar measurements of Arctic cirrus clouds

Veronika Wolf¹, Peter Voelger², Thomas Kuhn¹, Marin Stanev³, Jörg Gumbel³

(1) Luleå University of Technology, Division of Space Technology, Kiruna, Sweden

(2) Swedish Institute of Space Physics (IRF), Solar Terrestrial and Atmospheric Research Programme, Kiruna, Sweden

(3) Stockholm University, Department of Meteorology (MISU), Stockholm, Sweden

Cirrus clouds play an important role in the radiation balance of the Earth's atmosphere. Depending on their cloud and particle properties, the effect can be either warming or cooling. Of particular interest is cloud research in high latitudes, as to that point fewer measurements have been carried out there compared to other latitudes and this area is particularly affected by climate change.

To investigate the cloud and particle properties of Arctic cirrus, balloon-borne measurements, accompanied by LIDAR measurements, were carried out in Kiruna, northern Sweden. The payload for the balloon is an in-situ imager that takes photos of ice particles directly in the cloud and a radiosonde for temperature and humidity. Two LIDAR systems can measure concurrently, one directly at the launch site in ESRANGE and one about 30 km west of the launch site at the Swedish Institute of Space Physics.

The aim of these measurements is to use the advantages of both measuring principles and to gain the greatest possible knowledge through synergies with such joint measurements in order to improve, for example, satellite retrievals, and weather and climate models.

In this presentation we will focus on one recent campaign from earlier this year. We will compare the in-situ and LIDAR measurements with the main focus on extinction, depending on particle size, shape, and number concentration and discuss in which way both techniques complement each other.

Meteors

Invited

The Canadian Automated Meteor Observatory: high resolution studies of meteor ablation

M. Campbell-Brown¹, D. Subasinghe¹, D. Vida², T. Armitage¹

(1) University of Western Ontario, Department of Physics and Astronomy, London ON N6A 3K7 Canada, Margaret.campbell@uwo.ca

(2) University of Western Ontario, Department of Earth Sciences, London ON N6A 3K7 Canada

The Canadian Automated Meteor Observatory consists of three sets of optical systems, each at two sites located 45 km apart to enable triangulation. One of the systems, the tracking system, uses a pair of mirrors mounted on orthogonal axes and driven by high-speed galvanometers to direct the light from meteors detected in a wide-field camera into a small telescope. This system can resolve fragments of millimetre to centimetre sized meteoroids separated by distances of meters.

Most meteoroids in the mm to cm size range fragment (Subasinghe et al., 2016), most into a large number of fragments which cannot be resolved individually, but form a long luminous wake behind the meteor head. Even meteoroids with no distinguishable fragments or bright wake cannot be explained as single body objects (Campbell-Brown 2017), implying that even these are shedding small fragments as they ablate. A few of these minimally fragmenting objects produce light curves with double peaks, the cause of which may be multiple mineral compositions or strengths in a single meteoroid.

In cases where individual fragments are visible, the height of fragmentation can be inferred, which allows the maximum strength of the objects to be estimated. The evidence suggests that small meteoroids of this size have very weak strengths, consistent with weak contact forces among grains. Even when fragments cannot be individually resolved, the brightness and length of the wake of the meteor may be used to constrain the fragment distribution: this will allow better estimates of meteoroid parameters such as density.

Simultaneous observations of fragmenting meteoroids with the CAMO tracking system and with the multi-frequency CMOR radar will allow fragmentation to be taken into account in scattering models, which should improve models of the initial radius bias in radar observations.

Campbell-Brown, M., 2017. P&SS 143, 34.

Subasinghe, D., Campbell-Brown, M., Stokan, E. 2016, MNRAS 457, 1289.

Poster

A Monte-Carlo type simulation toolbox for small body dynamical astronomy

D. Kastinen^{1,2}, J. Kero¹, Asta Pellinen-Wannberg^{1,2}, Mats Holmström¹,
Jeremie Vaubaillon³, Urban Brändström¹

(1) Swedish Institute of Space Physics (IRF), Box 812, SE-98128 Kiruna, Sweden
(daniel.kastinen@irf.se)

(2) Umeå University, Department of Physics, SE-90187 Umeå, Sweden

(3) IMCCE, Observatoire de Paris, 61 Avenue de l'Observatoire, 75014 Paris, France

Earth is bombarded daily by billions of dust-sized particles amounting to around 4-200 tonnes of extraterrestrial material. Those larger than a few tenths of a millimetre give rise to visible streaks of light on the night sky: meteors. It is still an open question how much extra-terrestrial material enters the Earth's atmosphere. Meteoroids are a unique link between a phenomena occurring in the Earths atmosphere, the meteor, and astronomical bodies, the parent of the meteoroid.

Our project will carry out Monte Carlo type statistical simulations using high performance computing to investigate the mass propagation of material from parent bodies to Earth. A first case study to prototype the concept has been performed, comparing radar and visual observations of the 2011-2012 October Draconids [1].

The developed software toolbox will be published as open source and designed for reuse. Simulations will be compared to observational data from spacecraft and ground based instruments, such as the Middle and Upper Atmosphere (MU) radar in Japan, the current EISCAT system, the new EISCAT 3D facility and optical instruments. The simulations will provide calibrations to analyse measurements and with proper uncertainty analysis, data can be used as initial condition for the simulations.

[1] D. Kastinen, J. Kero. "A Monte Carlo-type simulation toolbox for Solar System small body dynamics: Application to the October Draconids." In: Planetary and Space Science (2017).

Regular

Simultaneous radar head echo and optical meteor observations

J. Kero⁽¹⁾, D. Kastinen⁽¹⁾, G. Stober⁽²⁾, C. Schult⁽²⁾, P. Brown⁽³⁾, Z. Krzeminski⁽³⁾, R. Marshall⁽⁴⁾, W. Cooke⁽⁵⁾ and I. Häggström⁽⁶⁾

(1) Swedish Institute of Space Physics (IRF), Box 812, SE-98128 Kiruna, Sweden, kero@irf.se

(2) Leibniz-Institute of Atmospheric Physics (IAP), Kühlungsborn, Germany

(3) University of Western Ontario, London, Ontario, Canada

(4) University of Colorado, Boulder, Colorado, USA

(5) NASA Meteoroid Environment Office, Marshall Space Flight Center, Huntsville, AL, USA

(6) EISCAT Scientific Association, Kiruna, Sweden

The meteoroid population has different characteristics at different mass scales, which means that an accurate mass range determination is needed to usefully compare observations of directionality, velocity distribution and flux obtained with different systems. However, there are significant uncertainties in the calculation of both photometric and ionization masses of meteors, not least in the study of low-mass meteoroids through meteor head echoes observations using high power, large aperture radars. While simultaneous radar and optical observations as such cannot be used to absolutely calibrate either the photometric or radar scattering mass scales, they are useful for determining the relative validity of the two scales. Simultaneous radar and optical observations are important also to better constrain the role of fragmentation.

We report efforts to obtain simultaneous radar head echo - optical meteor events and present a recent study using the MAARSY radar (53.5 MHz) simultaneously with the EISCAT UHF radar (930 MHz) and optical systems temporarily deployed at two locations, one at the ALOMAR observatory about 2 km from MAARSY and the other 15 km to the south. The EISCAT UHF radar is located 129 km to the east-northeast and was pointed at elevation 37° and azimuth 257° towards a measurement volume at 100 km altitude in zenith above MAARSY. The observations enable estimating meteor plasma parameters using a recently-developed two-frequency inversion technique, which is based on physical modeling of the radar scattering from the meteor plasma.

Invited

Optical Observations of Faint Meteors with a Wide-Field CMOS Camera Tomo-e Gozen

R. Ohsawa¹, S. Sako¹, F. Usui², Y. Sarugaku³, M. Sato⁴, Y. Fujiwara⁵, T. Ootsubo⁶, S. Abe⁷, A. Hirota⁷, K. Arimatsu⁸, T. Kasuga⁸, J. Watanabe⁸, and Tomo-e Gozen project members

(1) Institute of Astronomy, Graduate School of Science, The University of Tokyo, 181-0015, 2-21-1 Osawa, Mitaka, Tokyo, Japan, ohsawa@ioa.s.u-tokyo.ac.jp

(2) Center for Planetary Science, Graduate School of Science, Kobe University

(3) Koyama Astronomical Observatory, Kyoto Sangyo University

(4) The Nippon Meteor Society

(5) SOKENDAI (The Graduate University for Advanced Studies)

(6) Department of Space Astronomy and Astrophysics, Institute of Space and Astronautical Science (ISAS), Japan Aerospace Exploration Agency (JAXA)

(7) Department of Aerospace Engineering, College of Science and Technology, Nihon University

(8) National Astronomical Observatory of Japan

The interstellar dust particles (IDPs) are small members of the **sololar(solar)** system small bodies. The IDPs are rapidly (up to a few thousand years) removed by a radiation pressure or the Poynting-Robertson effect. Thus, the size distribution of the IDPs reflects the activity of the current solar system. The IDPs of between $\sim 0.1 \mu\text{g}$ to $\sim 1 \text{g}$ are difficult to investigate by in-situ observations or remote sensing. Instead, an IDP entering the Earth interacts with terrestrial atmosphere, causing a meteor phenomenon. The mass of the IDP can be indirectly measured by estimating the magnitude of the phenomenon.

Optical observations are widely used to measure the brightness of a meteor, which is a good indicator of the meteor mass. The meteor luminosity function constrains the mass distribution function of IDPs around the Earth. The luminosity function of meteors brighter than about 8 mag in the V-band has been well investigated. To observe faint meteors, a combination of a large aperture and wide-field telescope and a high-sensitive video camera. We have developed a wide-field CMOS mosaic camera, Tomo-e Gozen, for the 1.0-m Schmidt telescope at Kiso Observatory, the University of Tokyo. Tomo-e Gozen is designed to have 84 newly-developed CMOS sensors, to cover a ~ 20 square-degree sky at up to 2 Hz. A clear optical broad-band filter, peaking at about 5500 Å, is installed. A limiting magnitude for fixed stars in 2 Hz observations is about 18.5 mag in the V-band, corresponding to a limiting magnitude for meteors of about 13 mag. More than 2,000 meteors are expected to be detected by Tomo-e Gozen. We confirmed the sensitivity of the system with a prototype model of Tomo-e Gozen in 2015. In February 2018, we successfully carried out commissioning observations with one of four camera modules (21 CMOS sensors). In April 2018, coordinated observations were carried out with MU radar, RISH, Kyoto University. We'll introduce the results obtained in the observations with the prototype and the commissioning observations. We also plan slitless spectroscopic observations of faint meteors. Tomo-e Gozen will provide unique data sets of faint meteors to investigate IDPs around the Earth.

Active experiments in the upper atmosphere

Invited

A combined spectroscopic and plasma chemical kinetic analysis of ionospheric samarium releases

J. M. Holmes¹, R. A. Dressler², T. R. Pedersen¹, R. G. Caton¹, D. Miller¹

(1) Space Vehicles Directorate, Air Force Research Laboratory, Kirtland Air Force Base, New Mexico, USA

(2) Spectral Sciences, Incorporated, Burlington, Massachusetts, USA

Two rocket-borne releases of samarium vapor in the upper atmosphere occurred in May 2013, as part of the Metal Oxide Space Clouds experiment. The releases were characterized by a combination of optical and RF diagnostic instruments located at the Roi-Namur launch site and surrounding islands and atolls. The evolution of the optical spectrum of the solar-illuminated cloud was recorded with a spectrograph covering a 400–800 nm spectral range. The spectra exhibit two distinct spectral regions centred at 496 and 636 nm within which the relative intensities change insignificantly. The ratio between the integrated intensities within these regions, however, changes with time, suggesting that they are associated with different species. With the help of an equilibrium plasma spectral model, we attribute the region centred at 496 nm to neutral samarium atoms (Sm I radiance) and features peaking at 649 nm to a molecular species. No evidence for structure due to Sm⁺ (Sm II) is identified. The persistence of the Sm I radiance suggests a high dissociative recombination rate for the chemi-ionization product, SmO⁺. A one-dimensional plasma chemical kinetic model of the evolution of the density ratio $N_{\text{SmO}}/N_{\text{Sm}}(t)$ demonstrates that the molecular feature peaking at 649 nm can be attributed to SmO radiance. SmO⁺ radiance is not identified. By adjusting the Sm vapor mass of the chemical kinetic model input to match the evolution of the total electron density determined by ionosonde data, we conclude that less than 5% of the payload samarium was vaporized.

Invited

Spatial Separation of Optical Spectral Features in Chemical Release Experiments

T. Pedersen¹, J. Holmes¹, R. Caton¹

(1) Air Force Research Laboratory Space Vehicles Directorate, AFRL/RVBX 3550 Aberdeen Ave. SE, Kirtland AFB, NM, 87117, USA

Chemical releases in the upper atmosphere produce strong optical signatures when the cloud is sunlit but instruments can be operated in darkness on the ground below. Barium clouds are particularly well known for having neutral and ionized components distinguished by different fluorescence spectra, which also separate spatially due to the difference between neutral and plasma dynamics. Multi-spectral observations have been made during several recent releases of samarium during twilight, and show a small but distinct separation between blue and red components of the emissions and a very complex emission spectrum across the visual range between 400 and 700 nm. Initial analysis of the clouds lumped all emission bands together to obtain an average picture of cloud shape, size, and motion. We present spectra and narrow-band emission images of clouds from 3 rocket experiments at equatorial and middle latitudes and dusk and dawn local times and describe the differences between clouds viewed in the red and blue parts of the spectrum. We interpret the spatial separation of the spectral features in terms of atomic and molecular neutrals and ions.

Ground-based, in-situ and space-based instruments, new facilities

Poster

Russian ionosphere monitoring system based on GNSS data

V. Alpatov¹, P. Budnikov¹, A. Vasiliev¹

(1) Federal State Budgetary Institution Institute of Applied Geophysics.

Ionosphere monitoring is important not only for ionosphere research, but also for navigation and communication applications. GNSS receivers can provide ionosphere measurements of total electron content and scintillation level. Russian ionosphere monitoring network has more than 130 active GNSS station evenly distributed over the country. Significant part of the network is placed in a polar and sub-polar region, including 6 station on the Kola Peninsula. This network provides data for real-time monitoring system and 3D ionosphere tomography system. The real-time ionosphere monitoring system produces maps of total electron content - TEC, amplitude scintillation indexes, phase scintillation indexes, rate of TEC, rate of TEC intensity change and critical frequency fof2 every second with processing latency 30 ms. Fof2 are obtained from TEC measurements with ionosondes data assimilation. The 3-D tomography system provides 3D distribution of electron content every hour with latency about 20 minutes. Full meta data and results of computation have been continuously archived since 2011 year and allows to study long-term changes and trends in the ionosphere.

Invited

Laser investigation of the mesospheric magnetic field - The Mesospheric Sodium Layer as a Remotely, Optically Pumped Magnetometer

N. Gulbrandsen¹, M. G. Johnsen¹, J. Matzka², U.-P. Hoppe³, A. Serrano³, P. D. Hillman⁴, C.A. Denman⁴

(1) UiT the Arctic University of Norway, Tromsø Geophysical Observatory, Tromsø, Norway

(2) Helmholtz-Zentrum Potsdam, Deutsches GeoForschungsZentrum GFZ, Germany

(3) UiT the Arctic University of Norway, Department of Physics and Technology, Tromsø, Norway

(4) FASORtronics LLC, Albuquerque, NM, USA.

By means of optical pumping, it is possible to use the naturally occurring sodium layer in the mesosphere to measure Earth's scalar magnetic field at 90 km above ground. This is an altitude not accessible by other means than rockets, which only will provide point measurements of very short time scales. We are working to establish a sodium lidar system at ALOMAR in Northern Norway to be capable, for the first time, to measure and monitor the magnetic field in situ in the high latitude mesosphere over longer time scales. The technique, which has been proposed earlier for measurements at low or mid-latitudes for studies of Earth's internal magnetic field, will in our project be applied to high latitudes in the auroral zone. This opens for a completely new domain of measurements of externally generated geomagnetic variations related to currents in the magnetosphere-ionosphere system.

In particular, we aim to measure the magnetic field variations in close vicinity to Birkeland currents associated with particle precipitation events penetrating to altitudes below 90 km and small-scale, discrete auroral arcs. It is, furthermore, anticipated that it will be possible to detect horizontal current structures in the E-layer on much smaller length scales than it is presently possible from ground observations alone. During the project, we plan take advantage of the rich space science infrastructure located in northern Norway, including ALOMAR, EISCAT and the Tromsø Geophysical Observatory magnetometer network. If possible, we also aim to make measurements in conjunction with overpasses of the SWARM satellites.

Invited

ALOMAR Tropospheric Lidar – Developments and ongoing projects

Ingrid Hanssen¹, Michael Gausa¹

(1) Andøya Space Center, Bleiksvæien 46, N-8480 Andenes, Norway, ingrid@andoyaspace.no

The Arctic Lidar Observatory for Middle Atmosphere Research (ALOMAR) is a full-scale atmospheric observatory located at Andøya (69N, 16E) managed by Andøya Space Center (ASC). The observatory opened in 1994, and is still developing in terms of new instruments and own research.

The tropospheric lidar, owned by ASC is operational since 2005. The system is a three-wavelength elastic backscatter lidar with Raman and depolarization capabilities. ALOMAR is a member of the European Aerosol Research Lidar Network (EARLINET) and partner in the EU H2020 project ACTRIS-2. Co-located with the lidar is a CIMEL 318-T photometer operated by the Atmospheric Optics Group at the University of Valladolid. The tropospheric lidar and photometer are intended as a national facility in the European Research Infrastructure ACTRIS, currently on the ESFRI roadmap. This will involve further upgrades and changes to the lidar-system to deliver a comprehensive dataset.

ALOMAR participates in the calibration and validation (Cal/Val) activities for both Adm-Aeolus (launch August 21st, 2018), Sentinel-5P (launched October 13th, 2017) and EarthCARE (launch 2020), providing valuable data on aerosol and cloud-properties. In addition, co-located photometer data and radio soundings from a nearby radiosonde station are utilized in the validation.

Regular

Japanese Space-Earth Coupling Exploration Mission by Multiple Polar-orbiting Compact Satellites and its Collaborations in Instrumentations and Ground-based Observations

Masafumi Hirahara¹, Yoshifumi Saito², Hirotsugu Kojima³, and Masatoshi Yamauchi⁴

(1) Institute for Space-Earth Environmental Research, Nagoya University, Nagoya, Japan

(2) Institute of Space and Astronautical Science, Japan Aerospace Exploration Agency, Sagami-hara, Japan

(3) Research Institute of Sustainable Humanosphere, Kyoto University, Uji, Japan

(4) Swedish Institute of Space Physics, Kiruna, Sweden

After the successful launch and the recent observational progresses of the ERG(Arase) satellite mission, we have been leading the next exploration mission in the Japanese space physics research community, called FACTORS (Frontiers of formation, Acceleration, Coupling, and Transport mechanisms Observed by outer space Research System). Consisting of polar orbiting multi-satellite team, the ground-based observation teams, and the modellings/simulation teams, FACTORS is targeting the space-Earth connection system responsible for the formations and couplings of the various transition regions and processes, and the acceleration and transportation mechanisms of the space plasma and neutral atmospheric particles in the magnetosphere-ionosphere-thermosphere. FACTORS will quantitatively elucidate numerous unclear processes and mechanisms by using the demonstrative in-situ observations with the cutting-edge measurement techniques for plasma particle/waves and electric/magnetic fields and also the remote-sensing observations of the atmospheric emissions like auroras by monochromatic imaging cameras onboard FACTORS launched around 2025 by a Synergy Epsilon rocket of JAXA. The FACTORS mission will consist of two or three similar compact satellites and keep a peculiar type of sun-synchronous orbit in the noon-midnight meridian with altitudes from 300 km (targeted perigee) to 4000 km (apogee) while the initial perigee altitude would be around 400 km for avoiding significant air drag effects in the initial critical operation phase and the close formation flight phase. It is also evident that the instrumental and observational collaborations with the overseas space agencies/institutes and the ground-based observation facilities would bring us with more advanced and fruitful results. The science objectives, the observational methodology, and the mission strategies, and the international collaboration plans of FACTORS are given in this presentation.

Regular

Detection of infrasound in the Earth's upper atmosphere by observing nightglow emissions

Julianne Kealy¹, Frank Mulligan¹

(1) Maynooth University, Collegeland, Maynooth, Co. Kildare, Ireland, julianne.kealy@mu.ie

A small 3-element array of radiometers has been deployed at Maynooth University (53.4°N,6.6°W) to search for evidence of infrasonic waves at mesopause altitudes as part of a ARISE 2020 collaborative effort to investigate atmospheric dynamics. Infrasound is known to be generated by a variety of sources in the troposphere, including volcanic eruptions, mine explosions, nuclear detonations and earthquakes. The very low attenuation of these acoustic frequencies as a function of altitude means that they propagate vertically more or less unhindered to the OH* layer near ~87 km altitude. Pressure variations from these waves should increase or decrease the number of emitting OH* radicals in a fixed volume of atmosphere and thereby modulate the quantity of infrared light emitted from that volume. Radiometers sensitive to these emitted wavelengths may be capable of detecting such modulations during the hours of darkness, where the resulting data can be analysed using FFT and wavelet analysis. Ongoing ionospheric scintillation measurements at a number of UK universities may provide additional evidence for these propagating acoustic waves in the upper atmosphere.

Poster

A quantitative analysis of high-speed time-resolved spectroscopy of sparks recorded by GALIUS

N. Kieu¹, M. Passas¹, J. Sánchez¹ and F. J. Gordillo-Vázquez¹

(1) Instituto de Astrofísica de Andalucía (IAA-CSIC), Glorieta de la Astronomía s/n, 18008 Granada, Spain, kieuuny@iaa.es

We describe GALIUS (GrAnada Lightning Ultrafast Spectrograph) and present some preliminary spectra recordings of 5 - 10 cm long sparks created by a small electrostatic (30 – 300 kV) generator in our laboratory. GALIUS is an extremely sensitive, ultrafast and high spectral resolution spectrograph developed at the IAA - CSIC designed to operate as a portable groundbased scientific instrument supporting the Atmosphere Space Interaction Monitor (ASIM) mission of ESA (launched last April 2, 2018) and the future TARANIS and Meteosat Third Generation (MTG) Lightning Imager (LI) space missions to track atmospheric electricity from space.

GALIUS uses four interchangeable volume holographic phase (VHP) diffraction grating working in the near ultraviolet, visible and near-infrared spectral range. For each VHP, GALIUS records spark images with recording speeds varying from 20 kfps (frames per second) up to more than 2 Mfps. GALIUS is triggered by a fast photometer monitoring the first light emitted by the spark.

We now present preliminary results corresponding to GALIUS operation within the visible and near infrared optical ranges working at spectral and temporal resolutions of, respectively, 0.42 nm, 1 nm, up to 0.5 μ s (recording speed of 2.1 Mfps). When operating in the visible range, using a VHP centered at 657.3 nm, the recorded spark spectra exhibited a rich temporal dynamics of the H α line (656.3 nm) that last for almost 5 μ s after the triggering of the spark. In the near infrared spectral range, using a VHP centered at 775 nm, the recorded spectral images show the time evolution of the neutral oxygen triplet at 777 nm up to 6 μ s. When recording at 40000 fps, the above mentioned spectral features are observed until almost 25 μ s. When the visible range is explored with a VHP centered at 621 nm (and a spectral resolution of 1 nm) the spark spectra exhibits the presence of several "early" atomic nitrogen ion lines originated 1.5 μ s before triggering that were recorded thanks to the continuous GALIUS buffer mode (it saves a designated number of frames before trigger).

We present our first estimations of the electron density and temperature derived from time-resolved spark spectra using Stark line broadening and assuming Boltzmann equilibrium.

Invited

GRASSP and GALIUS: two slit spectrographs designed to remotely characterize transient atmospheric plasmas

M. Passas¹, N. Kieu¹, J. Sánchez¹ and F. J. Gordillo-Vázquez¹ O.Van der Velde², J.Montanyá²

(1) Instituto de Astrofísica de Andalucía (IAA-CSIC), Glorieta de la Astronomía sn, 18008 Granada, Spain, passasv@iaa.es

(2) Department of Electrical Engineering, Universitat Politècnica de Catalunya, Barcelona, Spain

We present the main parameters and design features of GRASSP and GALIUS instruments, two slit spectrographs designed, developed and built by our group, intended to remotely characterize transient atmospheric plasmas.

GRASSP (GRAnada Sprite Spectrograph and Polarimeter) is an iCCD spectrograph provided with a 1440 grooves/mm grating, planned for the analysis of the faint optical emissions of transient luminous events (TLEs), by terms of measuring the spectra of the light emitted from these fast optical phenomena with a spectral resolution of 0.25 nm and a dispersion of 0.07 nm/px in the wavelength range between 700 and 800 nm. It is currently installed in Castellgalí (Barcelona, Spain) and provides data as a ground support to space missions ASIM (ESA), which was successfully launched last 2nd April 2018, and TARANIS (CNES) to be launched by late 2019.

On the other hand, GALIUS (GrAnada Lightning Ultrafast Spectrograph) is a CMOS spectrograph provided with a set of four different volume phase holographic (VPH) gratings, intended to carry out high-speed lightning and spark spectroscopy campaigns, with a spectral resolution from 0.42 nm to 1 nm and a dispersion from 0.14 nm/px to 0.33 nm/px, depending on the grating. GALIUS can work in the near-ultraviolet (NUV) (360 – 400 nm), visible (VIS) (400 – 700 nm) and near-infrared (NIR) (700 – 850 nm) spectral range thanks to a set of modular UV and VIS-NIR optical elements. Using a sensor size of 1024 x 8 pixels GALIUS is able to achieve frame rates above 900 Kfps and goes over 2 Mfps under reduced (128 x 8 pixels) sensor size. Such high recording speed is of interest to explore extreme temporal dynamics of key spectroscopic lines revealing the behaviour of electric fields, electron density and temperature during different lightning and spark phases.

Invited

SS-520-3 Sounding Rocket Experiment Targeting the Ion Outflow over the Cusp Region

Y. Saito¹, Y. Ogawa², H. Kojima³, and SS-520-3 Sounding Rocket Experiment Team

(1) Institute of Space and Astronautical Science, 3-1-1 Yoshinodai, Chuo, Sagami-hara, Kanagawa 252-5210, Japan, saito@stp.isas.jaxa.jp

(2) National Institute of Polar Research, Tachikawa, Tokyo, Japan

(3) Research Institute for Sustainable Humanosphere, Kyoto University, Uji, Kyoto, Japan

In order to achieve collective understanding of the microphysics and its role (scale coupling) in the global to meso scale phenomena in the polar ionosphere, Japan-Norway sounding rocket experiment program is now in progress. The first ISAS sounding rocket in this program is SS-520-3 planned to be launched from Ny-Ålesund, Svalbard in Spitsbergen. The main objective of this sounding rocket is to understand the particle acceleration processes that cause the ion outflow by making in-situ observation of the wave-particle interaction over the dayside cusp region.

SS-520-3 sounding rocket experiment aims to resolve the wave-particle interaction by making in-situ measurement over the polar cusp region with newly developed instruments for the satellite mission. Since these wave-particle interactions are predicted to be effective above 800km altitude, a two-stage sounding rocket SS-520 whose apex can be higher than 800km is necessary. The rocket range where SS-520 can be launched over dayside cusp is only Ny-Ålesund in Svalbard. Since simultaneous ground based optical observation of the cusp aurora is necessary to decide the launch timing, the best launch period is determined from the conditions of both the sunlight and the moonlight. From the sunlight condition, the best launch period is in the winter polar night that is around the winter solstice. On the other hand, two weeks before/after the new moon is the best launch period from the condition of the moonlight. Launch window for each day is 0700UT-1130UT (0800LT-1230LT: 1000MLT-1430MLT) when the cusp is possibly on the same magnetic field line as the trajectory of SS-520-3.

SS-520-3 sounding rocket experiment is a part of the comprehensive observation campaign including ground-based radar and optical observations. SS-520-3 sounding rocket experiment is also one of the projects participating to “A Grand Challenge Initiative (GCI) Cusp program” that is a large-scale international collaboration for targeting advancement in the common understanding of cusp region space physics.

Although SS-520-3 was planned to be launched in December 2017, the launch was postponed at least by one year due to mal-function of the timer equipment that was found during the final stage of the integration test. The timer equipment problem has already been completely fixed. However, another problem is endangering the earliest launch of SS-520-3 in winter 2018-2019. Since the budgetary situation at ISAS in 2018 is quite severe, launching SS-520-3 in winter 2018-2019 is difficult. Approaching the solar minimum that will be in 2020 in this solar cycle, the opportunities that satisfy the launch condition will decrease since the latitude of cusp becomes higher comparing the apex latitude of SS-520-3. SS-520-3 Payload Instrument team strongly hopes to launch SS-520-3 as early as possible.

Poster

FACTORS: A future satellite mission for understanding the coupling and transportation processes in the upper atmosphere

T. Sakanoi¹, M. Hirahara², M. Yamauchi³, K. Asamura⁴, Y. Saito⁴, Shin-ichiro Oyama^{2,5,6}, H. Kojima⁷, N. Kitamura⁹, Yuichi Tsuda⁸, A. Matsuoka⁴, Y. Miyoshi², K. Hosokawa⁸, N. Yagi¹, M. Fuiizawa¹

(1) Tohoku University, Sendai, Japan, tsakanoi@pparc.gp.tohoku.ac.jp

(2) ISEE, Nagoya University, Nagoya, Japan

(3) IRF, Kiruna, Sweden

(4) ISAS/JAXA, Sagamihara Japan

(5) University of Oulu, Oulu, Finland

(6) National Institute of Polar Research, Tachikawa, Japan

(7) RISH, Kyoto University, Kyoto, Japan

(8) University of Electro-Communications, Chofu, Japan

(9) The University of Tokyo, Tokyo, Japan

(7) University of Oulu, Oulu, Finland

(8) National Institute of Polar Research, Tachikawa, Japan

We report a future satellite mission which will aim to understand the coupling processes in the terrestrial magnetosphere/ionosphere/thermosphere and the acceleration and transportation of the space plasma and neutral atmospheric particles. This mission is called FACTORS (Frontiers of Formation, Acceleration, Coupling, and Transport Mechanisms Observed by Outer Space Research System) and this will be a community exploration mission in Japanese **apace(space)** research after the success of the ERG mission. We mainly concern on optical and ultra-violet remote sensing of aurora and airglow for this mission. A visible imager on FACTORS will measure small-scale auroral structures at a wavelength of auroral prompt emission line with high-time (~0.1s) and high-spatial (~1km) resolutions using EMCCD. The FOV of 8 x 8 deg covers an area of 400 x 400 km viewed from altitudes of 3000 km. The far-ultraviolet (FUV) imager adopts a wide (~50 x 50 deg.) FOV objective mirror system which covers ~3000 x 3000 km area viewed from 3000 km altitude. FUV imager adopts a filter wheel to change the wavelength between O 135.6 nm and the N₂ LBH band at 140-160 nm to estimate O/N₂ ratio. Wide-field N₂ image enable us to examine large-scale auroral dynamics like westward-travelling surge during substorm, and O/N₂ images provide us to understand the global thermospheric activity.

In addition, we are now carrying out two sounding rocket projects, Rocksats-XN/PARM and LAMP, and auroral image will install on the rockets. PARM on the Rocksats-XN rocket which will be launched from Andøya, Norway in January 2019. In this rocket mission, we carry out simultaneous auroral imaging and medium- and high-energy particle measurements to understand the generation and loss process of high-energy electrons associated with pulsating aurora (PsA). The auroral imaging camera (AIC) will measure the optical thickness and imaging of PsA. AIC consists of sensor (AIC-S) and electronics (AIC-E). AIC-S adopts a commercial-based wide field-of-view lens (FOV of 96 deg x 75 deg), RG-665 filter, and CCD (WAT-910HX). AIC-E will make CCD pixel binning to gain the sensitivity, and reduce the data telemetry. We completed the detailed design of AIC, and will fabricate by summer of 2018.

Regular

The DIY hyperspectral imager experiment

F. Sigernes¹, M. Syrjäso¹, R. Storvold², J. Fortuna³, M. E.Grøtte³, J. Veisdal³,
E. Honoré-Livermore³ and T. A. Johansen³

(1) University Centre in Svalbard (UNIS), N-9171 Longyearbyen, Norway (freds@unis.no)

(2) Northern Research Institute, Tromsø, Norway.

(3) Norwegian University of Science and Technology, Trondheim, Norway

Rapid prototype construction of small and lightweight push broom Hyper Spectral Imagers (HSI) is presented. The dispersive element housings are printed by thermoplastic 3D printers combined with off-the-shelf optical mechanical components and camera heads. Five models are described with a spectral range in the visible to the near-infrared part of the electromagnetic spectrum. The bandpass is in the range from 1 - 5 nm. Test experiments with motorized gimbals to stabilize attitude show that the instruments are capable of spectral imaging from various platforms, including airborne drone to handheld operations. The main aim is to adapt and use this technology in space.

Invited

The Investigation of Cusp Irregularities 5 sounding rocket: multi-point measurement of turbulence

A. Spicher¹, J. I. Moen¹, H. Hoang¹, K. Røed¹, E. Trondsen¹, L. B. N. Clausen¹,
W. J. Miloch¹,

(1) Department of Physics, University of Oslo, Oslo, Norway

Plasma turbulence and irregularities are common in the high latitude F region ionosphere. The irregular density structures spanning a few meters to a few kilometers are of significant importance for space weather applications, as they can create scintillations and degrade the quality of Global Navigation Satellite Systems (GNSS) signals and high frequency (HF) radio communication. In order to develop forecast models of GNSS space weather there is a need to understand the underlying physics, which mainly involve plasma instabilities, waves, and turbulence.

The Investigation of Cusp Irregularities (ICI) sounding rocket program has been developed to investigate the formation of scintillation irregularities in the Polar Regions and to assess the mechanisms responsible for them. Thanks to the ICI program and to the high-resolution density measurements allowed by the multi-needle Langmuir probe system on-board the sounding rockets, significant progress have been made in the past few years. However, these density measurements being one dimensional, they do not allow to determine the spatial extent of the irregularities, nor do they provide any unambiguous answer regarding energy transfer between the different scales, which is essential to understand the underlying physics. To overcome these issues multi-point measurements are necessary. This will be achieved by the ICI-5 sounding rocket, the Norwegian contribution to the Grand Challenge Initiative - Cusp (<https://www.andoyaspace.no/the-grand-challenge-initiative/>). The ICI-5 will carry two 4DSpace modules from which a total of 12 “daughter payloads” measuring electron density will be ejected. This will provide critical knowledge about the spatial extend of scintillation irregularities, and allow to explore and characterize the nature of plasma turbulence in the cusp ionosphere.

Regular

Coordinated satellite and ground-based observations of fast atmospheric processes.

R. Vasilyev¹, A. Beletsky¹, A. Bogomolov², M. Kaznacheeva³, P. Klimov², E. Komarova⁴, A. Mikhalev¹, R. Rakhmatulin¹, S. Podlesny¹, I. Tkachev¹

(1) Institute of Solar-Terrestrial Physics SB RAS, Russia, 664033, Irkutsk p/o box 291; Lermontov st., 126a, roman_vasilyev@iszf.irk.ru

(2) Skobeltsyn institute of nuclear physics, Lomonosov Moscow State University

(3) Physical department, Lomonosov Moscow State University

(4) Physical department, Irkutsk State University

We present complex of instruments and preliminary results for coordinated satellite and ground based observations of the fast geophysical events due to atmospheric electricity, fast auroral and airglowing processes, meteors etc. The potential of such kind research is in additional possibility to recognize the relations between the geophysical processes in atmosphere-ionosphere-magnetosphere system with integration of local and global observational systems, but using additional proxies. The fast geophysical processes usually characterised by fast energy transfer and make very bright signatures, especially in the optical traces. The global variations of such events under different geomagnetic or meteorologic conditions could give us additional information about variability of the physical, chemical and electrical structure of the atmosphere.

Regular

Development of a near-infrared balloon-borne camera for dayside and sunlit auroral observations

Xiaoyan Zhou^{1,2} and S. B. Rafol³

(1) Department of Earth, Planetary, and Space Sciences, University of California, Los Angeles, California, USA, xyzhou@igpp.ucla.edu

(2) XYZ Space Physics, Inc., Pasadena, California, USA

(3) Jet Propulsion Laboratory, Pasadena, California, USA

In the last hundred years, we have accumulated ample knowledge about nightside aurorae occurring during magnetic storms and magnetospheric substorms. In contrast, we know little about dayside aurorae, especially when they are in sunlight, which is the case more than 80% of the time. However, the dayside is particularly interesting because it is where the solar wind-magnetosphere-ionosphere coupling is initiated. Imaging aurora in daylight is a difficult and challenging task. The brightness of the sunlit atmosphere overwhelms the auroral emissions at visible wavelengths. Modeling of atmospheric brightness suggests that the contrast between auroral brightness and sky brightness makes it possible to image the aurora at near-infrared (NIR) wavelengths from sufficient altitudes. Preliminary experiments confirmed that the auroral N_2^+ Meinel emissions at ~ 1100 nm are bright enough to be extracted from atmospheric background brightness during daylight at about 40 km of a balloon altitude, which leads to the development of a high-performance NIR InGaAs camera that can be flown on a high-altitude and long-duration balloon. Aiming at weak auroral signals, the new camera maintains very low noise by cooling the detector to suppress the dark current noise and by employing a narrow bandpass filter to significantly reduce the sky background noise. In addition, the camera is a system with low mass, low power consumption, and relatively small scale in dimension. Auroral observations from such a platform can address some interesting and important questions, including: How do the dayside auroral features relate to the dayside solar wind-magnetosphere-ionosphere coupling? How do the dayside auroral features relate to nightside auroral features? And what are the hemispherical asymmetries in the aurora when one hemisphere is in the sunlight and the other is in the dark? The balloon-based observations, which are highly accommodated to current space missions (such as THEMIS/ARTEMIS, MMS, Cluster, Geotail, DMSP, and AMPERE) and many ground-based measurements, provide a unique opportunity for conjugate auroral investigations when the balloon flights are conducted at both southern and northern hemispheres and/or when the imaging from the Antarctic balloon coordinates with the ground-based auroral observations around the arctic winter solstice. Furthermore, when the balloon can be launched together with an auroral investigation rocket (such as from ESRANGE, Sweden), the science return will be enhanced significantly.

EISCAT-3D and optical instruments

Regular

ALIS_4D, a Swedish complementary instrument for EISCAT_3D, status of Kiruna Atmospheric and Geophysical Observatory and the European Working group on optical calibration.

U. Brändström¹, the ALIS_4D team^{1,2}, the KAGO team¹ and the EWOC team^{1,3}

(1) Swedish Institute of Space Physics, Kiruna, Sweden

(2) Department of Physics, University of Umeå

(3) Many other places. (Full author lists with affiliations given in the presentation)

This paper presents three related status reports: (1) ALIS_4D, a Swedish complementary instrument for EISCAT_3D (2) Kiruna Atmospheric- and Geophysical Observatory (KAGO) and (3) the European working group on optical calibration (EWOC).

ALIS_4D (www.alis4d.irf.se) is a joint effort between IRF and Umeå University to provide a high-performance low-light optical multi-station imaging facility replacing ALIS. The system will use the same infrastructure as ALIS but is equipped with modern EMCCD imagers providing considerable higher temporal resolution as well as long-term monitoring capabilities in addition to the 3D-reconstruction abilities already present in ALIS. Four new imagers together with optical systems (FoV about 150°) has already been delivered and ALIS_4D is planned to begin operations in the fall of 2019. The system will be compatible with corresponding facilities in Finland and Norway.

At IRF **KAGO** has the responsibility for ALIS_4D, EWOC and other standard long-term monitoring instruments such as: magnetometers, all-sky cameras, ionosondes, riometers, infrasound detection as well as measurements of trace-gases in the atmosphere. A short overview indicating planned upgrades, future prospects and possibilities with respect to EISCAT_3D are given.

EWOC (www.alis.irf.se/ewoc) has since many years had the responsibility of the intercalibration workshops of light-standards (calibrators) intended for calibration of low-light optical instrumentation (such as the ALIS and ALIS_4D imagers). The time series for the Fritz Peak reference source dates back to 1967. All other light-standards are compared with the reference during the intercalibration workshops. The last intercalibration workshop was in Sodankylä September 2016 and an intercalibration workshop is also planned during the 45AM.

Regular

EISCAT 3D: overview of the system and its experiment modes

C.-F. Enell¹, H. Hellgren¹, C. J. Heinselman¹, A. Westman¹ and J. Markkanen²

(1) EISCAT Scientific Association, Box 812, SE-98128 Kiruna, Sweden

(2) Sodankylä Geophysical Observatory, Tähteläntie 62, FIN-99600 Sodankylä, Finland

The EISCAT 3D construction project has started with an official kickoff event in September 2017, and we are currently working on site preparation, procurements of electronic and mechanical parts, design of control software, etc.

This talk is intended to give an overview of the most important aspects of EISCAT 3D, in order to aid developers and operators of complementary ground-based optical instruments to design and operate their systems, and to serve as a background to discussions among those research groups.

Topics to consider include

- software and data flow
- suggested experiment modes
- user interfaces for experiment design and request

Invited

EISCAT_3D Capabilities and Status

C. Heinselman¹

(1) EISCAT Scientific Association, Rymdcampus 1, Kiruna, Sweden, craig.heinselman@eiscat.se

The EISCAT_3D Implementation project is finally under way, after more than a decade of planning and design work. Over that time, the available technologies have changed quite substantially, and the system being built will have many capabilities not initially envisioned. Some of these capabilities will be especially interesting for collaborative studies with other existing and hoped-for instrumentation in the region (especially optical systems).

This presentation will show what the radar will be able to do, what some of its limitations will be, and where the project is in terms of the overall time line.

Regular

New insights found from coalescence of the ionospheric and thermospheric measurements at auroral latitudes

S. Oyama^{1,2,3}, M. G. Conde⁴, A. Aikio², E. Turunen⁵, K. Kauristie⁶, H. Vanhamäki², I. Virtanen², U. Brändström⁷, T. Ulich⁵, L. Cai², A. Workayehu², K. Shiokawa¹, M. Ishii⁸, M. Hirahara¹, T. Sakanoi⁹, Y. Tanaka³, C. Fallen⁴, B. J. Watkins⁴, M. Orispää², and Y. Ogawa³

- (1) ISEE, Nagoya U., Japan
- (2) U. Oulu, Finland
- (3) NIPR, Japan
- (4) GI UAF, USA
- (5) SGO, U. Oulu, Finland
- (6) FMI, Finland
- (7) IRF, Sweden
- (8) NICT, Japan
- (9) Tohoku U., Japan

Understanding the flow of energy and mass throughout the magnetosphere-ionosphere-thermosphere coupled system is a fundamental goal of solar-terrestrial physics. Substantial energy accumulated in the substorm growth phase in the magnetospheric tail primarily flows into the polar ionosphere immediately after the substorm onset, resulting in notable fluctuations in the polar ionosphere and thermosphere. However, at the growth and recovery phases, the polar ionosphere and thermosphere show variations characterized by the phase-dependent features. Investigating the energy dissipation process at high latitudes at each substorm phase can contribute significantly to achieving that fundamental goal mentioned above.

In this talk, we introduce representative signatures in the polar thermosphere and ionosphere by comparing with auroral morphological changes, mainly based on ground-based measurements such as cameras, Fabry-Perot interferometer and incoherent scatter radar. This presentation will also discuss future researching plans, in particular regarding application of EISCAT_3D, Scanning Doppler Imagers (SDIs) and the FACTORS satellite.

Regular

Optical and other ground-based instrumentation: readiness for EISCAT_3D

Th. Ulich¹, S. Oyama^{2,3}, U. Brändström⁴, K. Kauristie⁵, B. Gustavsson⁶, and C. Hall⁷

(1) Sodankylä Geophysical Observatory, Sodankylä, Finland

(2) ISEE, Nagoya University, Japan

(3) Ionospheric Physics Group, University of Oulu, Oulu, Finland

(4) Swedish Institute of Space Physics, Kiruna, Sweden

(5) Finnish Meteorological Institute, Helsinki, Finland

(6) Dept of Physics and Technology, UiT – The Arctic University of Norway, Tromsø, Norway

(7) Tromsø Geophysical Observatory, UiT – The Arctic University of Norway, Tromsø, Norway

The EISCAT_3D radar is expected to be built by 2022. The new radar will have only limited scientific value without a comprehensive and well-organised network of optical and other ground-based observations. Currently, ground-based instrumentation in the Nordic countries is disjunct and operated by a number of Nordic institutes, which additionally host a number of guest instruments contributed from all over the world.

In order to get the maximum benefit from EISCAT_3D, there is urgent need to have well-co-ordinated ground-based observations. The timeline of EISCAT_3D constructions sets a clear deadline to achieve this, and the first steps are being taken by the newly-established Nordic Observatory Collaboration, of which currently TGO, KAGO, FMI, and SGO are part and others are welcome to join.

It has been suggested to establish a roadmap, i.e. a plan, for the development of optical and other instrumentation during the EISCAT_3D construction phase in order to prepare ourselves for the new radar becoming operational. This roadmap should, however, not stop there, but instead look ahead towards the next 10 to 15 years, during which we will also need to address the future of ESR and the Heater.

Here we will discuss these future opportunities and challenges. We will present concrete steps that have been proposed so far and share our vision of future joint radar and ground-based operations from the point of view of Nordic Observatories.

Author index

Aikio A. University of Oulu, Oulu, Finland	70
Alpatov V. Fedorov Institute of Applied Geophysics Roscomhydromet, Russia	10, 53
Ansmann A. Leibniz Institute for Tropospheric Research (TROPOS), Leipzig, Germany	39
Arimatsu K. National Astronomical Observatory of Japan, Japan	48
Armitage T. University of Western Ontario, Department of Earth Sciences, London, Canada	45
Artamonov, M. Institute of Solar-Terrestrial Physics SB RAS, Irkutsk, Russia	21, 31
Asamura K. ISAS/JAXA, Sagamihara Japan	61
Bag T. Swedish Institute of Space Physics, Kiruna, Sweden	7
Barinova V. Skobeltsyn Institute of Nuclear Physics, Moscow State University, Moscow, Russia	33
Belakhovsky V.B. Polar Geophysical Institute, Apatity, Russia	8
Beletsky A. Institute of Solar-Terrestrial Physics SB RAS, Irkutsk, Russia	21, 64
Blindheim S. ALOMAR Observatory, Andøya Space Center, Andenes, Norway	41
Bogomolov V. Skobeltsyn Institute of Nuclear Physics, Moscow State University, Moscow, Russia	33, 36, 64
Bolmgren K. University of Bath, UK	16
Brändström U. Swedish Institute of Space Physics, Kiruna, Sweden	6, 23, 46, 67, 70, 71
Brown P. University of Western Ontario, London, Ontario, Canada	47
Budnikov P. Kaliningrad department of IZMIRAN, Kaliningrad, Russia	10,53
Cachorro V. Group of Atmospheric Optics, University of Valladolid, Spain	41
Cai L. University of Oulu, Oulu, Finland	70
Calle A. Group of Atmospheric Optics, University of Valladolid, Spain	41
Campbell-Brown M. University of Western Ontario, Department of Physics and Astronomy, London, Canada	45
Caton R. Space Vehicles Directorate, Air Force Research Laboratory, Kirtland Air Force Base, New Mexico, USA	50, 51

Chadney J. University of Southampton, UK	17, 22, 26
Chernous S. Polar Geophysical Institute, Murmansk, Russia	10
Chernyakov S. Polar Geophysical Institute, Apatity, Russia	28
Christensen O. Department of Meteorology (MISU), Stockholm University, Sweden	29
Clausen L. Department of Physics, University of Oslo, Oslo, Norway	9, 63
Conde M. GI UAF, USA	70
Cooke W. NASA Meteoroid Environment Office, Marshall Space Flight Center, Huntsville, AL, USA	47
Cremonini R. "A. Avogadro," University of Turin, Turin, Italy	36
Dahlgren H. Royal Institute of Technology (KTH), Stockholm, Sweden	22
Dalin, P. Swedish Institute of Space Physics, Kiruna, Sweden	27, 42
Dashkevich Zh.V. Polar Geophysical Institute, Apatity, Russia	11, 13
de Frutos A. Group of Atmospheric Optics, University of Valladolid, Spain	41
Denman C. FASORtronics LLC, Albuquerque, NM, USA	54
Devyatova E. Institute of Solar-Terrestrial Physics SB RAS, Irkutsk, Russia	31
Dressler R. Spectral Sciences, Incorporated, Burlington, Massachusetts, USA	50
Efishov I. Kaliningrad department of IZMIRAN, Kaliningrad, Russia	10
Enell C.-F. EISCAT Scientific Association, Kiruna, Sweden	68
Fallen C. GI UAF, USA	70
Fear R.C. Department of Physics and Astronomy, University of Southampton, UK	18
Filatov, M. Polar Geophysical Institute, Murmansk, Russia	10
Fortuna J. Norwegian University of Science and Technology, Trondheim, Norway	62
Freudenthaler V. Ludwig-Maximilians-Universität, Meteorological Institute, München, Germany	39
Fuiizawa M. Tohoku University, Sendai, Japan	61
Fujiwara Y. SOKENDAI (The Graduate University for Advanced Studies), Japan	48
Garipov G. Skobeltsyn Institute of Nuclear Physics, Moscow State University, Moscow, Russia	33, 36

Gasteiger J. University of Vienna, Aerosol Physics and Environmental Physics, Wien, Austria	39
Gausa M. ALOMAR Observatory, Andøya Space Center, Andenes, Norway	41, 55
González R. Group of Atmospheric Optics, University of Valladolid, Spain	41
Gordillo-Vázquez F. Instituto de Astrofísica de Andalucía (IAA-CSIC), Granada, Spain	58, 59
Groß S. German Aerospace Center (DLR), Institute of Atmospheric Physics, Wessling, Germany	39
Grøtte M. Norwegian University of Science and Technology, Trondheim, Norway	62
Gulbrandsen N. UiT the Arctic University of Norway, Tromsø Geophysical Observatory, Tromsø, Norway	54
Gumbel J. Department of Meteorology (MISU), Stockholm University, Sweden	29, 43
Gustavsson B. UiT, the Arctic University of Norway, Tromsø Norway	11, 14, 71
Häggström I. EISCAT Scientific Association, Kiruna, Sweden	27, 47
Hall C. Tromsø Geophysical Observatory, UiT – The Arctic University of Norway, Tromsø, Norway	71
Hanssen I. ALOMAR Observatory, Andøya Space Center, Andenes, Norway	41, 55
Hedin J. Department of Meteorology (MISU), Stockholm University, Sweden	30
Heinselmann C. EISCAT Scientific Association, Kiruna, Sweden	68, 69
Hellgren H. EISCAT Scientific Association, Kiruna, Sweden	68
Herreras M. Group of Atmospheric Optics, University of Valladolid, Spain	41
Hillman P. FASORtronics LLC, Albuquerque, NM, USA	54
Hirahara M. Institute for Space-Earth Environmental Research, Nagoya University, Nagoya, Japan	56, 61, 70
Hirota A. Department of Aerospace Engineering, College of Science and Technology, Nihon University, Japan	48
Hoang H. Department of Physics, University of Oslo, Oslo, Norway	63
Holmes J. Space Vehicles Directorate, Air Force Research Laboratory, Kirtland Air Force Base, New Mexico, USA	50, 51
Holmström M. Swedish Institute of Space Physics, Kiruna, Sweden	46
Honoré-Livermore E. Norwegian University of Science and Technology, Trondheim, Norway	62
Hoppe U.-P. UiT the Arctic University of Norway, Department of Physics and Technology, Tromsø, Norway	54

Hosokawa K. University of Electro-Communications, Chofu, Japan	61
Ishii M. NICT, Japan	70
Ivanov V.E. Polar Geophysical Institute, Apatity, Russia	
Ivchenko N. Royal Institute of Technology (KTH), Stockholm, Sweden	22, 29
Janghede, M. Department of Meteorology (MISU), Stockholm University, Sweden	29
Jin Y. Department of Physics, University of Oslo, Oslo, Norway	7
Johnsen M. UiT the Arctic University of Norway, Tromsø Geophysical Observatory, Tromsø, Norway	54
Juusola, L. Finnish Meteorological Institute, Helsinki, Finland	15
Kadokura A. National Institute of Polar Research, Tokyo, Japan	16
Kastinen D. Swedish Institute of Space Physics, Kiruna, Sweden	46, 47
Kasuga T. National Astronomical Observatory of Japan, Japan	48
Kauristie K. Finnish Meteorological Institute, Helsinki, Finland	16, 70, 71
Kavanagh A.J. British Antarctic Survey, Cambridge, UK	18
Kaznacheeva M. Skobeltsyn Institute of Nuclear Physics, Moscow State University, Moscow, Russia Lomonosov Moscow State University, Moscow, Russia	36, 64
Kealy J. Maynooth University, Ireland	22, 57
Kero J. Swedish Institute of Space Physics, Kiruna, Sweden	46, 47
Khrenov B. Skobeltsyn Institute of Nuclear Physics, Moscow State University, Moscow, Russia	36
Kieu N. Instituto de Astrofísica de Andalucía (IAA-CSIC), Granada, Spain	58, 59
Kitamura N. The University of Tokyo, Tokyo, Japan	61
Klimenko M. Institute of Solar-Terrestrial Physics SB RAS, Irkutsk, Russia	21
Klimov P. Skobeltsyn Institute of Nuclear Physics, Moscow State University, Moscow, Russia	34, 35, 36, 64
Kojima H. Research Institute of Sustainable Humanosphere, Kyoto University, Uji, Japan	56, 60, 61
Komarova E. Physical department, Irkutsk State University	64
Kosé S. Kyoto University, Japan	23

Kozelov B.V. Polar Geophysical Institute, Apatity, Russia	13
Krzeminski Z. University of Western Ontario, London, Ontario, Canada	47
Kuhn T. Luleå University of Technology, Division of Space Technology, Kiruna, Sweden	43
Kvammen A. UiT, the Arctic University of Norway, Tromsø Norway	14
Lanchester B.S. Department of Physics and Astronomy, University of Southampton, UK	18, 22, 26
Latteck R. Leibniz-Institute of Atmospheric Physics, Kühlungsborn, Germany	27
Mann I. UiT the Arctic University of Norway, Tromsø, Norway	27
Markkanen J. Sodankylä Geophysical Observatory, Sodankylä, Finland	68
Marshall R. University of Colorado, Boulder, Colorado, USA	47
Mateos D. Group of Atmospheric Optics, University of Valladolid, Spain	41
Matsuoka A. ISAS/JAXA, Sagami-hara Japan	61
Matzka J. Helmholtz-Zentrum Potsdam, Deutsches GeoForschungsZentrum GFZ, Germany	54
McKay D. UiT, the Arctic University of Norway, Tromsø Norway	14
Medvedeva I. Institute of Solar-Terrestrial Physics SB RAS, Irkutsk, Russia	31
Megner L. Department of Meteorology (MISU), Stockholm University, Sweden	29
Merzlyakov E. Institute of experimental meteorology, Roshydromet, Obninsk, Russia	31
Mikhalev A. Institute of Solar-Terrestrial Physics SB RAS, Irkutsk, Russia	21, 31, 64
Miller D. Space Vehicles Directorate, Air Force Research Laboratory, Kirtland Air Force Base, New Mexico, USA	50
Miloch W. Department of Physics, University of Oslo, Oslo, Norway	8, 63
Miyoshi Y. ISEE, Nagoya University, Nagoya, Japan	61
Moen J. Department of Physics, University of Oslo, Oslo, Norway	63
Montanyà J. Polytechnic University of Catalonia, Terrassa, Spain	37
Mordvinov V. Institute of Solar-Terrestrial Physics SB RAS, Irkutsk, Russia	31
Mulligan F. Maynooth University, Ireland	22, 57
Murtagh D. Chalmers University of Technology, Göteborg, Sweden	29

Nakao K. Department of Physics, Meiji University, Kawasaki, Japan	40
Nickisch H. Philips Research, Hamburg, Germany	9
Nishi M. Hiroshima City University, Japan	23
Ogawa Y. National Institute of Polar Research, Tachikawa, Tokyo, Japan	60, 70
Ogloblina O. Polar Geophysical Institute, Apatity, Russia	28
Ohsawa R. Institute of Astronomy, The University of Tokyo, Tokyo, Japan	48
Ootsubo T. Department of Space Astronomy and Astrophysics, Institute of Space and Astronautical Science (ISAS), Japan Aerospace Exploration Agency (JAXA), Japan	48
Orispää M. University of Oulu, Oulu, Finland	70
Oyama S. ISEE, Nagoya University, Nagoya, Japan University of Oulu, Oulu, Finland National Institute of Polar Research, Tachikawa, Japan	61, 70, 71
Paavilainen T University of Helsinki, Helsinki, Finland	14
Panasyuk I. Skobeltsyn Institute of Nuclear Physics, Moscow State University, Moscow, Russia Lomonosov Moscow State University, Moscow, Russia	33, 36
Panasyuk M. Skobeltsyn Institute of Nuclear Physics, Moscow State University, Moscow, Russia	
Partamies N. UNIS University Centre in Svalbard, Svalbard, Norway, Birkeland Centre for Space Science, Bergen, Norway	14, 15, 16
Passas M. Instituto de Astrofísica de Andalucía (IAA-CSIC), Granada, Spain	58, 59
Pedersen T. Space Vehicles Directorate, Air Force Research Laboratory, Kirtland Air Force Base, New Mexico, USA	50, 51
Pellinen-Wannberg A. Umeå University, Department of Physics, Umeå, Sweden Swedish Institute of Space Physics, Kiruna, Sweden	46
Podlesny S. Institute of Solar-Terrestrial Physics SB RAS, Irkutsk, Russia	64
Pogoreltsev A. Russian State Hydrometeorological University, St. Petersburg, Russia	31
Price D. University of Southampton, UK	17
Rafol S. Jet Propulsion Laboratory, Pasadena, California, USA	65
Rakhmatulin R. Institute of Solar-Terrestrial Physics SB RAS, Irkutsk, Russia	64
Ratovsky K. Institute of Solar-Terrestrial Physics SB RAS, Irkutsk, Russia	21

Reidy J.A. Department of Physics and Astronomy, University of Southampton, UK British Antarctic Survey, Cambridge, UK	18
Røed K. Department of Physics, University of Oslo, Oslo, Norway	63
Roldugin A. Polar Geophysical Institute, Apatity, Russia	28
Roldugin V. Polar Geophysical Institute, Apatity, Russia	28
Román R. Group of Atmospheric Optics, University of Valladolid, Spain	41
Rourke S. Maynooth University, Ireland	22
Saito Y. Institute of Space and Astronautical Science, Japan Aerospace Exploration Agency, Sagami-hara, Japan	56, 60, 61
Sakanoi T. Tohoku University, Sendai, Japan	61, 70
Sako S. Institute of Astronomy, The University of Tokyo, Tokyo, Japan	48
Saleev K. Skobeltsyn Institute of Nuclear Physics, Moscow State University, Moscow, Russia	33
Sánchez J. Instituto de Astrofísica de Andalucía (IAA-CSIC), Granada, Spain	58, 59
Sarugaku Y. Koyama Astronomical Observatory, Kyoto Sangyo University, Japan	48
Sato M. The Nippon Meteor Society, Japan	48
Schult C. Leibniz-Institute of Atmospheric Physics (IAP), Kühlungsborn, Germany	47
Sergienko T. Swedish Institute of Space Physics, Kiruna, Sweden	7, 19, 23
Serrano A. UiT the Arctic University of Norway, Department of Physics and Technology, Tromsø, Norway	55
Shagimuratov I. Fedorov Institute of Applied Geophysics Roscomhydromet, Russia	10
Shiokawa K. ISEE, Nagoya University, Nagoya, Japan	70
Sigernes F. UNIS, Longyearbyen, Norway Birkeland Centre for Space Science (BCSS), University of Bergen, Norway The Kjell Henriksen Observatory, Svalbard, Norway Centre for Autonomous Marine Operations and Systems, NTNU, Norway	20, 62
Spicher A. Department of Physics, University of Oslo, Oslo, Norway	63
Stanev M. Stockholm University, Department of Meteorology (MISU), Stockholm, Sweden	43
Stegman, J. Department of Meteorology (MISU), Stockholm University, Sweden	29
Stober G. Leibniz-Institute of Atmospheric Physics (IAP), Kühlungsborn, Germany	47

Storvold R. Northern Research Institute, Tromsø, Norway	62
Subasinghe D. University of Western Ontario, Department of Physics and Astronomy, London, Canada	45
Suzuki H. Meiji University, Kawasaki, Kanagawa, Japan	30
Svertilov S. Skobeltsyn Institute of Nuclear Physics, Moscow State University, Moscow, Russia	33, 36
Syrjäsuo M. University Centre in Svalbard (UNIS), Longyearbyen, Norway	62
Tachikawa M. Department of Physics, Meiji University, Kawasaki, Japan	40
Tanaka Y. National Institute of Polar Research, Tachikawa, Japan	70
Tepenitsina N. Kaliningrad department of IZMIRAN, Kaliningrad, Russia	10
Tesche M. University of Herfordshire, Hatfield, United Kingdom	39
Tkachev I. Institute of Solar-Terrestrial Physics SB RAS, Irkutsk, Russia	64
Toledano C. Group of Atmospheric Optics, University of Valladolid, Spain	41
Trondsen E. Department of Physics, University of Oslo, Oslo, Norway	63
Tsuda Y. University of Electro-Communications, Chofu, Japan	61
Turunen E. Sodankylä Geophysical Observatory, Sodankylä, Finland	70
Ulich T. Sodankylä Geophysical Observatory, Sodankylä, Finland	70, 71
Usui F. Center for Planetary Science, Graduate School of Science, Kobe University, Japan	48
van der Velde O. Polytechnic University of Catalonia, Terrassa, Spain	37, 59
van Dijk D. The Hague University of Applied Science, The Netherlands	23
Vanhamäki H. University of Oulu, Oulu, Finland	70
Vasiliev A. Fedorov Institute of Applied Geophysics Roscomhydromet, Russia	53
Vasilyev R. Institute of Solar-Terrestrial Physics SB RAS, Irkutsk, Russia	21, 31, 64
Vaubailon J. IMCCE, Observatoire de Paris, Paris, France	46
Veisdal J. Norwegian University of Science and Technology, Trondheim, Norway	62
Velasco C. Group of Atmospheric Optics, University of Valladolid, Spain	41
Virtanen I. University of Oulu, Oulu, Finland	70

Voelger P. Swedish Institute of Space Physics, Kiruna, Sweden	42,43
Wandinger U. Leibniz Institute for Tropospheric Research (TROPOS), Leipzig, Germany	38
Watanabe J. National Astronomical Observatory of Japan, Japan	48
Watkins B. GI UAF, USA	70
Westman A. EISCAT Scientific Association, Kiruna, Sweden	68
Weygand J. University of California, Los Angeles, USA	15
Whiter D. University of Southampton, UK	16, 17, 18, 22, 26
Wintoft P. Swedish Institute of Space Physics, Lund, Sweden	23
Wirth M. German Aerospace Center (DLR), Institute of Atmospheric Physics, Wessling, Germany	39
Wolf V. Luleå University of Technology, Division of Space Technology, Kiruna, Sweden	43
Workayehu A. University of Oulu, Oulu, Finland	70
Yagi N. Tohoku University, Sendai, Japan	61
Yamashita R. Meiji University, Kawasaki, Kanagawa, Japan	30
Yamauchi M. Swedish Institute of Space Physics, Kiruna, Sweden	23, 56, 61
Zherebtsov G. Institute of Solar-Terrestrial Physics SB RAS, Irkutsk, Russia	21
Zhou X. Department of Earth, Planetary, and Space Sciences, University of California, Los Angeles, USA XYZ Space Physics, Inc., Pasadena, California, USA	24, 65
Zorkaltseva O. Institute of Solar-Terrestrial Physics SB RAS, Irkutsk, Russia	30



INSTITUTET FÖR RYMDFYSIK
Swedish Institute of Space Physics

Swedish Institute of Space Physics
Box 812, SE- 981 28 Kiruna, SWEDEN
tel. +46-980-790 00, fax +46-980-790 50, e-post: irf@irf.se

www.irf.se